Supporting Information

Non-cationic hyper-crosslinked ionic polymers with hierarchically ordered porous structures: facile synthesis and applications for highly efficient CO_2 capture and conversion

Bihua Chen, Junfeng Zeng, Shiguo Zhang* and Yan Zhang*

College of Materials Science and Engineering, Hunan University, Changsha 410082, Hunan, China

*Corresponding author.

E-mail addresses: zhangsg@hnu.edu.cn (S. Zhang), zyan1980@hnu.edu.cn (Y. Zhang).

1. Synthesis of the IL monomers

1.1. Synthesis of 1-methyl-3-ethylimidazolium bromide ([MEIm]Br) and 1-methyl-3-ethylimidazolium tetraphenylborate ([MEIm]BPh₄)
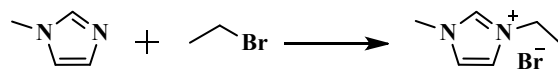
Scheme S1 Synthetic route of [MEIm]Br.

1-Methylimidazole (100 mmol) and bromoethane (110 mmol) were dissolved in 20 mL acetonitrile in a 100 mL round-bottom flask. The mixture was stirred at 40 °C for 24 h under an argon (Ar) atmosphere. After the reaction finished, the upper phase was removed, and the lower phase was washed with diethyl ether, and then dried under vacuum at 60 °C for 12 h. [MEIm]Br was obtained at a yield of approximately 96 % and was structurally characterized by NMR spectroscopy.

^{1}H NMR (400 MHz, CDCl$_3$, TMS) δ (ppm): 10.29 (s, 1H), 7.66 (s, 2H), 4.44 (q, J = 7.2 Hz, 2H), 4.13 (s, 3H), 1.62 (t, J = 7.4 Hz, 3H).
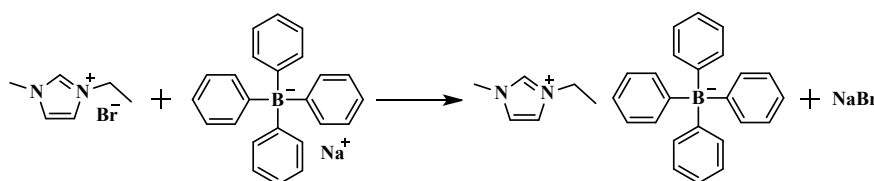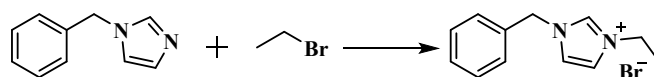

Scheme S2 Synthetic route of [MEIm]BPh₄.

[MEIm]Br (20 mmol) was dissolved in 50 mL deionized water in a 250 mL round-bottom flask. NaBPh$_4$ (22 mmol) was dissolved in 100 mL deionized water, and then dropped into the above solution. A precipitate was immediately formed, and the reaction mixture was stirred at room temperature for 24 h. The crude product was washed with excess deionized water several times and then dried under vacuum at 70 °C for 12 h. [MEIm]BPh$_4$ was obtained at a yield of approximately 94 % and was structurally characterized by NMR spectroscopy.

^{1}H NMR (400 MHz, DMSO-d$_6$, TMS) δ (ppm): 9.06 (s, 1H), 7.75 (s, 1H), 7.67 (s, 1H), 7.23–7.13 (m, 8H), 6.92 (t, J = 7.4 Hz, 8H), 6.79 (t, J = 7.0 Hz, 4H), 4.17 (q, J = 7.2 Hz, 2H), 3.82 (s, 3H), 1.40 (t, J = 7.2 Hz, 3H); ^{13}C NMR (100 MHz, DMSO-d$_6$,

TMS) δ (ppm): 164.58, 164.09, 163.60, 163.11, 136.63, 136.01, 125.83, 125.80, 125.78, 125.75, 124.03, 122.42, 122.00, 44.59, 36.14, 15.57.

1.2. Synthesis of 1-benzyl-3-ethylimidazolium bromide ([BnEIm]Br) and 1-benzyl-3-ethylimidazolium tetraphenylborate ([BnEIm]BPh$_4$)

Scheme S3 Synthetic route of [BnEIm]Br.[1]

1-Benzylimidazole (50 mmol) and bromoethane (52.5 mmol) were dissolved in 40 mL acetonitrile in a 100 mL round-bottom flask. The mixture was stirred at 80 ºC for 24 h under an Ar atmosphere. After the reaction finished, the upper phase was removed, and the lower phase was washed with diethyl ether until 1-benzylimidazole was not detected in the washing liquid by thin layer chromatography (TLC), and then dried under vacuum at 60 ºC for 12 h. [BnEIm]Br was obtained at a yield of approximately 82 % and was structurally characterized by NMR spectroscopy.

^{1}H NMR (400 MHz, DMSO-d$_6$, TMS) δ (ppm): 9.50 (s, 1H), 7.88 (s, 2H), 7.47–7.36 (m, 5H), 5.47 (s, 2H), 4.22 (q, J = 7.2 Hz, 2H), 1.42 (t, J = 7.4 Hz, 3H).
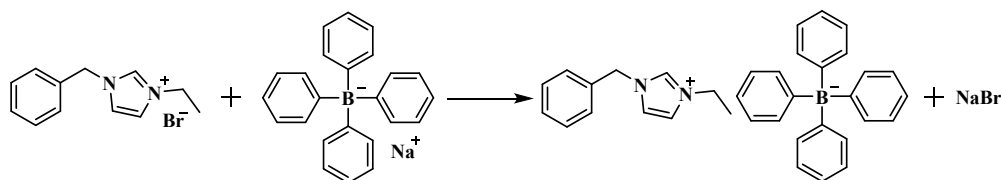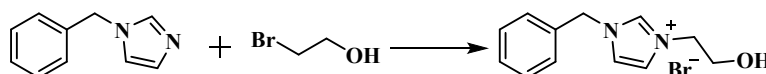

Scheme S4 Synthetic route of [BnEIm]BPh$_4$.

[BnEIm]Br (20 mmol) was dissolved in 50 mL deionized water in a 250 mL round-bottom flask. NaBPh$_4$ (22 mmol) was dissolved in 100 mL deionized water, and then dropped into the above solution. A precipitate was immediately formed, and the reaction mixture was stirred at room temperature for 24 h. The crude product was washed with excess deionized water several times and then dried under vacuum at 70 ºC for 12 h. [BnEIm]BPh$_4$ was obtained at a yield of approximately 96 % and was structurally characterized by NMR spectroscopy.

^{1}H NMR (400 MHz, DMSO-d$_6$, TMS) δ (ppm): 9.26 (s, 1H), 7.79 (d, J = 5.2 Hz, 2H), 7.45–7.39 (m, 5H), 7.23–7.15 (m, 8H), 6.93 (t, J = 7.2 Hz, 8H), 6.79 (t, J = 7.2 Hz, 4H), 5.39 (s, 2H), 4.18 (q, J = 7.2 Hz, 2H), 1.41 (t, J = 7.4 Hz, 3H); ^{13}C NMR (100 MHz, DMSO-d$_6$, TMS) δ (ppm): 164.56, 164.07, 163.58, 163.09, 136.26, 136.01, 134.41, 129.48, 129.22, 128.72, 127.04, 125.82, 125.79, 125.76, 125.74, 122.97, 121.99, 52.42, 44.81, 15.41.

1.3. Synthesis of 1-benzyl-3-(2-hydroxyethyl)imidazolium bromide ([BnHEIm]Br) and 1-benzyl-3-(2-hydroxyethyl)imidazolium tetraphenylborate ([BnHEIm]BPh$_4$)

Scheme S5 Synthetic route of [BnHEIm]Br.

1-Benzylimidazole (50 mmol) and 2-bromoethanol (52.5 mmol) were dissolved in 20 mL acetonitrile in a 100 mL round-bottom flask. The mixture was stirred at 80 ºC for 48 h under an Ar atmosphere. After the reaction finished, the upper phase was removed, and the lower phase was washed with diethyl ether until 1-benzylimidazole was not detected in the washing liquid by TLC, and then dried under vacuum at 60 ºC for 12 h. [BnHEIm]Br was obtained at a yield of approximately 94 % and was structurally characterized by NMR spectroscopy.

^{1}H NMR (400 MHz, DMSO-d$_6$, TMS) δ (ppm): 9.32 (s, 1H), 7.80 (d, J = 17.6 Hz, 2H), 7.46–7.36 (m, 5H), 5.46 (s, 2H), 5.19 (s, 1H), 4.24 (s, 2H), 3.73 (s, 2H).
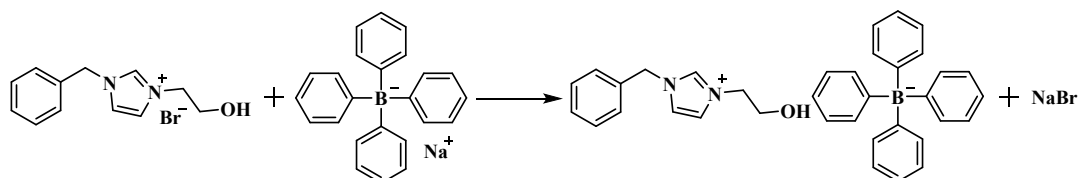

Scheme S6 Synthetic route of [BnHEIm]BPh$_4$.

[BnHEIm]Br (20 mmol) was dissolved in 50 mL deionized water in a 250 mL round-bottom flask. NaBPh$_4$ (22 mmol) was dissolved in 100 mL deionized water,

and then dropped into the above solution. A precipitate was immediately formed, and the reaction mixture was stirred at room temperature for 24 h. The crude product was washed with excess deionized water several times and then dried under vacuum at 70 ºC for 12 h. [BnHEIm]BPh$_4$ was obtained at a yield of approximately 92 % and was structurally characterized by NMR spectroscopy.

^{1}H NMR (400 MHz, DMSO-d$_6$, TMS) δ (ppm): 9.24 (s, 1H), 7.78 (s, 1H), 7.74 (s, 1H), 7.45–7.37 (m, 5H), 7.22–7.16 (m, 8H), 6.93 (t, J = 7.2 Hz, 8H), 6.80 (t, J = 7.0 Hz, 4H), 5.42 (s, 2H), 5.19 (s, 1H), 4.21 (t, J = 4.8 Hz, 2H), 3.75–3.70 (m, 2H); ^{13}C NMR (100 MHz, DMSO-d$_6$, TMS) δ (ppm): 164.55, 164.06, 163.57, 163.08, 136.94, 135.99, 135.34, 129.46, 129.20, 128.68, 125.80, 125.78, 125.75, 125.73, 123.63, 122.74, 121.98, 59.65, 52.30, 52.25.

1.4. Synthesis of 1-benzyl-3-(2,3-dihydroxypropyl)imidazolium bromide ([BnDHPIm]Br) and 1-benzyl-3-(2,3-dihydroxypropyl)imidazolium tetraphenylborate ([BnDHPIm]BPh$_4$)
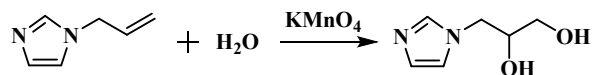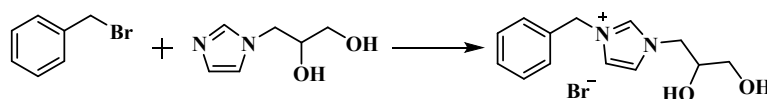

Scheme S7 Synthetic route of 3-(1H-imidazol-1-yl)propane-1,2-diol.[2]

1-Allylimidazole (46 mmol) was dissolved in 70 mL deionized water in a 500 mL round-bottom flask, and then cooled to 0 ºC. Potassium permanganate (KMnO$_4$, 46 mmol) was dissolved in 210 mL deionized water, cooled to 5 ºC, and then added to the above solution. The reaction mixture was stirred at 0 ºC for 4 h, and then in a boiling water bath for 1.5 h. After the reaction finished, the reaction mixture was filtered using a Buchner funnel, and the filtrate was collected. Deionized water was removed by using a rotary evaporator, and the residue was recrystallized from acetonitrile. 3-(1H-imidazol-1-yl)propane-1,2-diol was obtained at a yield of approximately 73 % and was structurally characterized by NMR spectroscopy.

^{1}H NMR (400 MHz, DMSO-d$_6$, TMS) δ (ppm): 7.56 (s, 1H), 7.12 (s, 1H), 6.86 (s, 1H), 4.81 (s, 2H), 4.07 (dd, J = 14.0 Hz, J = 3.6 Hz, 1H), 3.86 (dd, J = 14.0 Hz, J =

7.2 Hz, 1H), 3.70–3.64 (m, 1H), 3.34 (dd, J = 10.8 Hz, J = 4.8 Hz, 1H), 3.21 (dd, J = 10.8 Hz, J = 6.4 Hz, 1H).

Scheme S8 Synthetic route of [BnDHPIm]Br.

3-(1H-imidazol-1-yl)propane-1,2-diol (30 mmol) and benzyl bromide (30 mmol) were dissolved in 20 mL acetonitrile in a 100 mL round-bottom flask. The mixture was stirred at 80 ºC for 48 h under an Ar atmosphere. After the reaction finished, the upper phase was removed, and the lower phase was washed with diethyl ether until benzyl bromide was not detected in the washing liquid by TLC, and then dried under vacuum at 60 ºC for 12 h. [BnDHPIm]Br was obtained at a yield of approximately 78 % and was structurally characterized by NMR spectroscopy.

^{1}H NMR (400 MHz, DMSO-d$_6$, TMS) δ (ppm): 9.35 (s, 1H), 7.83 (s, 1H), 7.75 (s, 1H), 7.45–7.36 (m, 5H), 5.48 (s, 2H), 5.38–5.30 (m, 1H), 4.94 (s, 1H), 4.34 (dd, J = 13.6 Hz, J = 2.0 Hz, 1H), 4.11 (dd, J = 13.6 Hz, J = 8.0 Hz, 1H), 3.80 (s, 1H), 3.44 (dd, J = 10.8 Hz, J = 4.4 Hz, 1H), 3.27–3.23 (m, 1H).
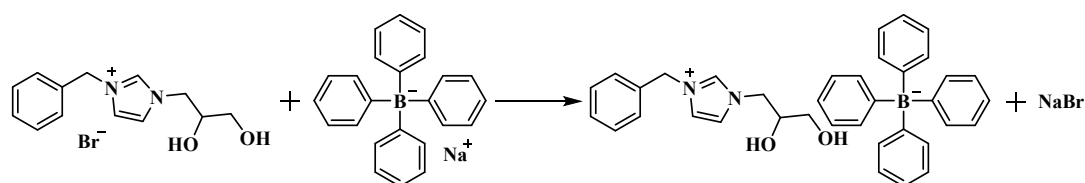
Scheme S9 Synthetic route of [BnDHPIm]BPh$_4$.

[BnDHPIm]Br (20 mmol) was dissolved in 50 mL deionized water in a 250 mL round-bottom flask. NaBPh$_4$ (22 mmol) was dissolved in 100 mL deionized water, and then dropped into the above solution. A precipitate was immediately formed, and the reaction mixture was stirred at room temperature for 24 h. The crude product was washed with excess deionized water several times and then dried under vacuum at 70 ºC for 12 h. [BnDHPIm]BPh$_4$ was obtained at a yield of approximately 88 % and was structurally characterized by NMR spectroscopy.

^{1}H NMR (400 MHz, DMSO-d$_6$, TMS) δ (ppm): 9.23 (s, 1H), 7.77 (s, 1H), 7.71 (s, 1H), 7.45–7.37 (m, 5H), 7.22–7.15 (m, 8H), 6.93 (t, J = 7.2 Hz, 8H), 6.79 (t, J = 7.0 Hz, 4H), 5.43 (s, 2H), 5.35 (d, J = 4.4 Hz, 1H), 4.95 (s, 1H), 4.31 (dd, J = 13.6 Hz, J = 2.0 Hz, 1H), 4.09 (dd, J = 13.6 Hz, J = 8.0 Hz, 1H), 3.78 (s, 1H), 3.46–3.40 (m, 1H), 3.29–3.21 (m, 1H); ^{13}C NMR (100 MHz, DMSO-d$_6$, TMS) δ (ppm): 164.55, 164.06, 163.57, 163.08, 137.21, 136.00, 135.36, 129.46, 129.19, 128.63, 125.81, 125.78, 125.75, 125.73, 124.18, 122.51, 121.98, 69.96, 63.22, 52.80, 52.29.

2. Synthesis of the non-cationic hyper-crosslinked porous ionic polymers (HCPIPs)

Table S1 Synthesis conditions and yields of the non-cationic HCPIPs.[a]

HCPIP sample	$[R_1R_2Im]Br$ (mmol)	$[R_1R_2Im]BPh_4$ (mmol)	Yield (%)
H-[MEIm]BPh$_4$-FDA	/	5.0	48
H-[BnEIm]BPh$_4$-FDA	/	5.0	57
H-[BnEIm]Br-FDA	5.0	/	≈ 0
H-[BnEIm]Br/BPh$_4$-FDA	2.5	2.5	58
H-[BnHEIm]BPh$_4$-FDA	/	5.0	53
H-[BnHEIm]Br-FDA	5.0	/	≈ 0
H-[BnHEIm]Br/BPh$_4$-FDA	2.5	2.5	52
H-[BnDHPIm]BPh$_4$-FDA	/	5.0	37
H-[BnDHPIm]Br-FDA	5.0	/	≈ 0
H-[BnDHPIm]Br/BPh$_4$-FDA	2.5	2.5	39

[a]Hyper-crosslinking conditions: 20 mmol FDA, 20 mmol FeCl$_3$, 20 mL 1,2-dichloroethane, stirred at 45 ºC for 3 h and 80 ºC for 21 h, Ar atmosphere.

3. Characterizations of the non-cationic HCPIPs

Table S2 Textural properties of the non-cationic HCPIPs.

HCPIP sample	S_{BET}^a $(m^2\ g^{-1})$	S_{micro}^b $(m^2\ g^{-1})$	S_{micro}/S_{BET}	V_{total}^c $(cm^3\ g^{-1})$
H-[MEIm]BPh$_4$-FDA	95	54	0.568	0.099
H-[BnEIm]BPh$_4$-FDA	137	72	0.526	0.146
H-[BnEIm]Br/BPh$_4$-FDA	729	350	0.480	0.591
H-[BnHEIm]BPh$_4$-FDA	121	68	0.562	0.117
H-[BnHEIm]Br/BPh$_4$-FDA	708	356	0.503	0.574
H-[BnDHPIm]BPh$_4$-FDA	116	53	0.457	0.123
H-[BnDHPIm]Br/BPh$_4$-FDA	636	319	0.502	0.483

[a]BET specific surface area.

[b]Microporous surface area, estimated by the t-plot method.

[c]Total pore volume.
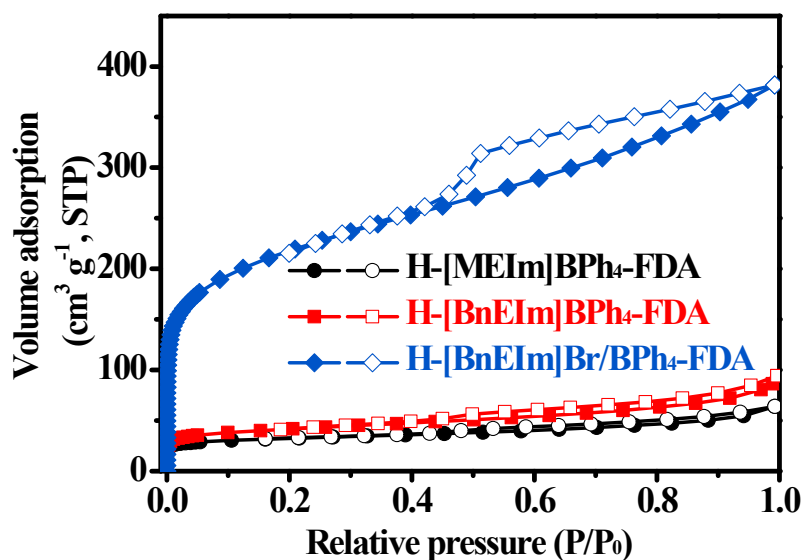
Figure S1 N$_2$ adsorption-desorption isotherms of H-[MEIm]BPh$_4$-FDA, H-[BnEIm]BPh$_4$-FDA, and H-[BnEIm]Br/BPh$_4$-FDA.
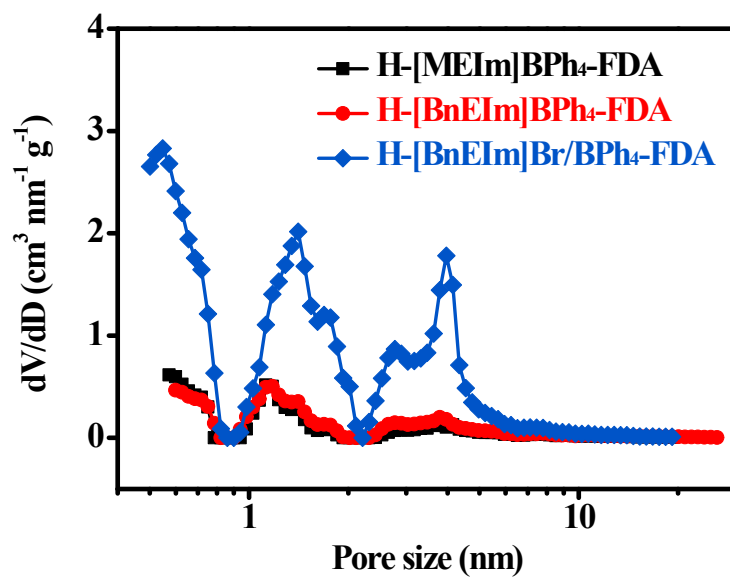
Figure S2 Pore size distributions of H-[MEIm]BPh$_4$-FDA, H-[BnEIm]BPh$_4$-FDA, and H-[BnEIm]Br/BPh$_4$-FDA.
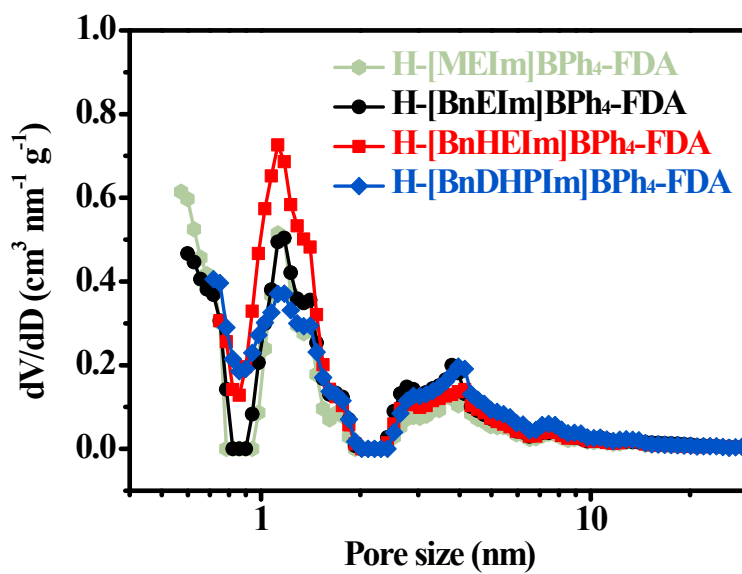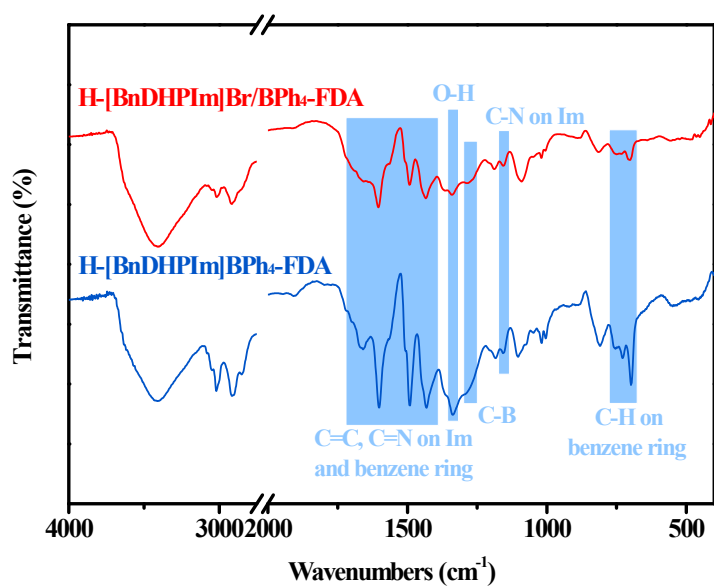

Figure S3 Pore size distributions of H-[MEIm]BPh$_4$-FDA, H-[BnEIm]BPh$_4$-FDA, H-[BnHEIm]BPh$_4$-FDA, and H-[BnDHPIm]BPh$_4$-FDA.
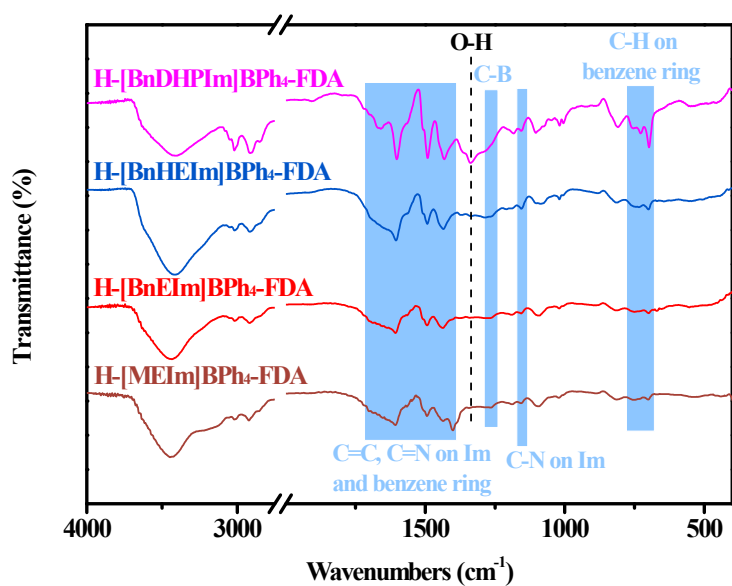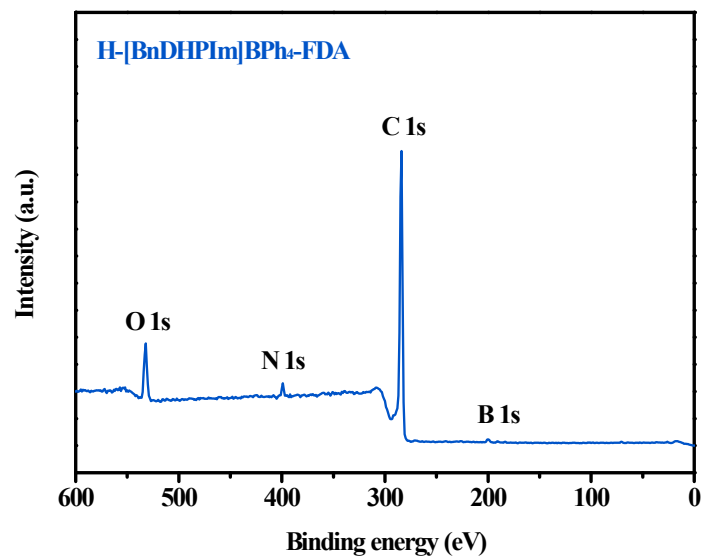
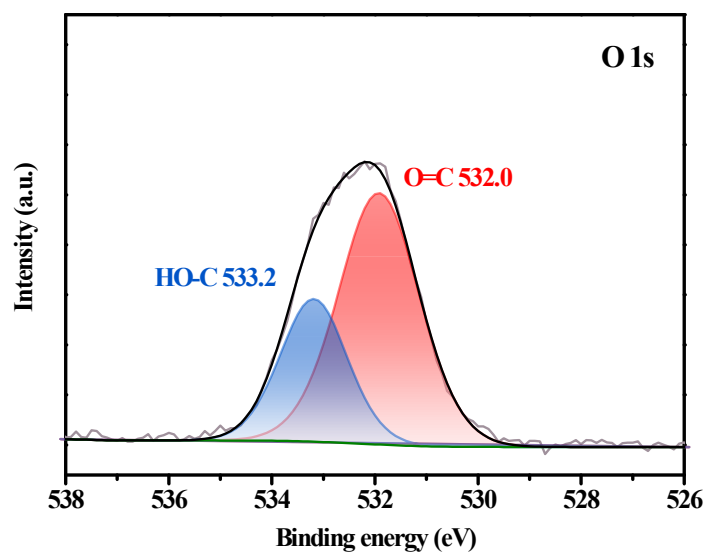**Figure S4** FT-IR spectra of H-[MEIm]BPh$_4$-FDA, H-[BnEIm]BPh$_4$-FDA, H-[BnHEIm]BPh$_4$-FDA, and H-[BnDHPIm]BPh$_4$-FDA.
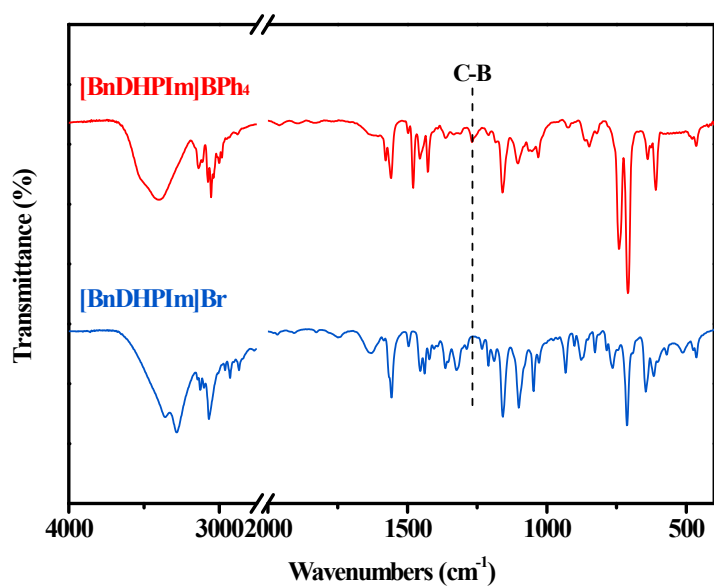
Figure S5 FT-IR spectra of [BnDHPIm]Br and [BnDHPIm]BPh$_4$.

Figure S6 FT-IR spectra of H-[BnDHPIm]BPh₄-FDA and H-[BnDHPIm]Br/BPh₄-FDA.

Figure S7 XPS spectrum of H-[BnDHPIm]BPh₄-FDA.

Figure S8 XPS measurement of O 1s spectrum over H-[BnDHPIm]Br/BPh₄-FDA.

Table S3 CHN elemental analysis, IL content, OH content, and B/Br molar ratio of the non-cationic HCPIPs.

HCPIP sample	C (wt%)	H (wt%)	N (wt%)	IL content[a] (mmol g⁻¹)	OH content[b] (mmol g⁻¹)	B/Br[c]
H-[BnEIm]Br/BPh₄-FDA	79.06	4.95	4.99	1.78	0	31.4
H-[BnHEIm]Br/BPh₄-FDA	77.41	4.85	4.71	1.68	1.68	35.4
H-[BnDHPIm]Br/BPh₄-FDA	75.90	4.86	3.35	1.20	2.40	38.8
H-[BnDHPIm]BPh₄-FDA	80.48	5.10	2.77	0.99	1.98	–

[a]IL content calculated by the N content, IL content = [N content] × 1000/(2 × 14).

[b]OH content = [IL content] × [number of OH group in IL monomer].

[c]B/Br molar ratio determined by the XPS.

**Table S4** Comparison of various HCPIPs between the specific surface area and IL content.

| Sample	S_{BET} (m^2 g^{-1})	IL content (mmol g^{-1})	Reference
H-[BnEIm]Br/BPh$_4$-FDA	729	1.78	**This work**
H-[BnHEIm]Br/BPh$_4$-FDA	708	1.68	**This work**
H-[BnDHPIm]Br/BPh$_4$-FDA	636	1.20	**This work**
POM3-IM	575	1.01	[3]
HIP-Br-2	534	0.30	[4]
NHC-CAP-1(Zn^{2+})	1040	1.51	[5]
CPIP-A-4	570	0.53	[6]
HPILs-Cl-2	500	0.88	[7]
IHCP-OH(1)	515	0.78	[8]
I$_{C2}$HCP-5b	1017	0.80	[9]
HP-[BZPhIm]Cl-DCX-1	763	0.732	[10]
Py-HCP-Br	435	0.76	[11]
IHCP-1	717	0.42	[12]
PIPs-5	520	1.20	[13]
HPMBr0.5	558	2.31	[14]
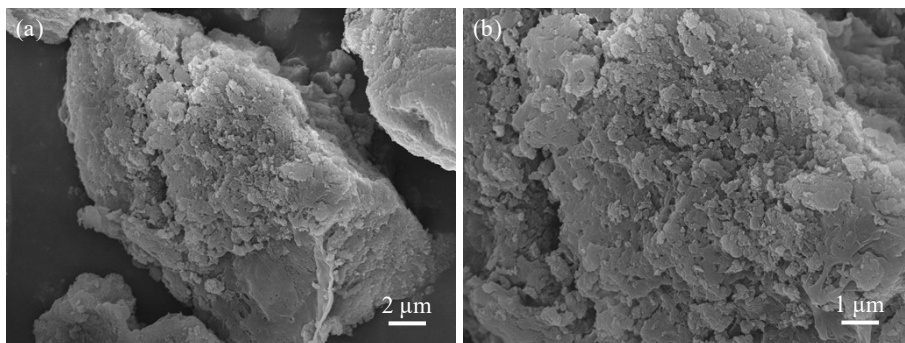
Figure S9 SEM images of H-[BnDHPIm]Br/BPh$_4$-FDA.
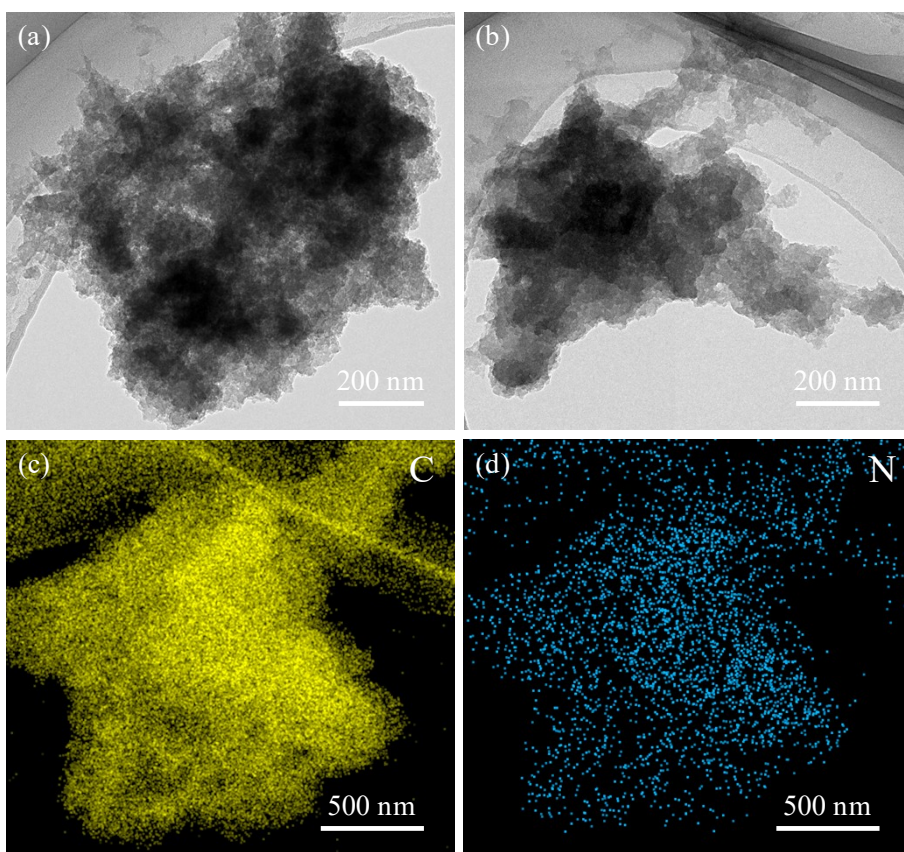
Figure S10 TEM images (a, b) and elemental (C and N) mapping images (c, d) of H-[BnDHPIm]Br/BPh$_4$-FDA.
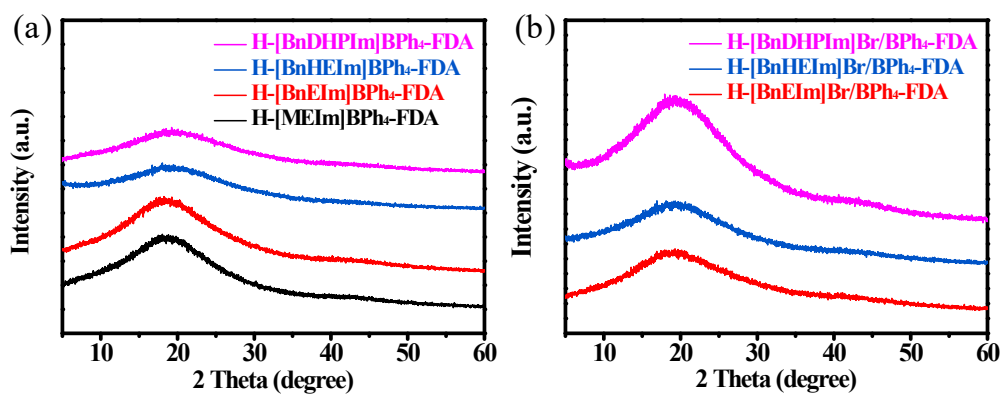
Figure S11 Powder XRD patterns of (a) H-[MEIm]BPh$_4$-FDA and H-[BnR$_2$Im]BPh$_4$-FDA, and (b) H-[BnR$_2$Im]Br/BPh$_4$-FDA. (R$_2$ = E, HE, and DHP)
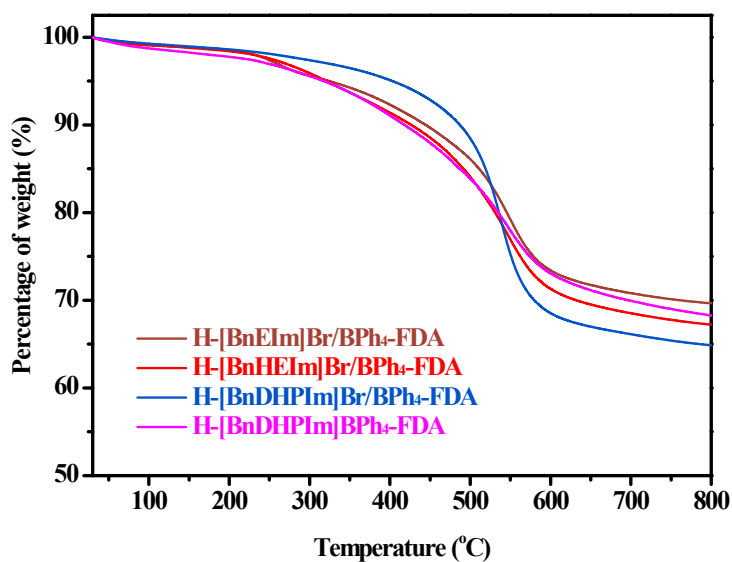
Figure S12 TGA curves of H-[BnR$_2$Im]Br/BPh$_4$-FDA (R$_2$ = E, HE, and DHP) and H-[BnDHPIm]BPh$_4$-FDA.
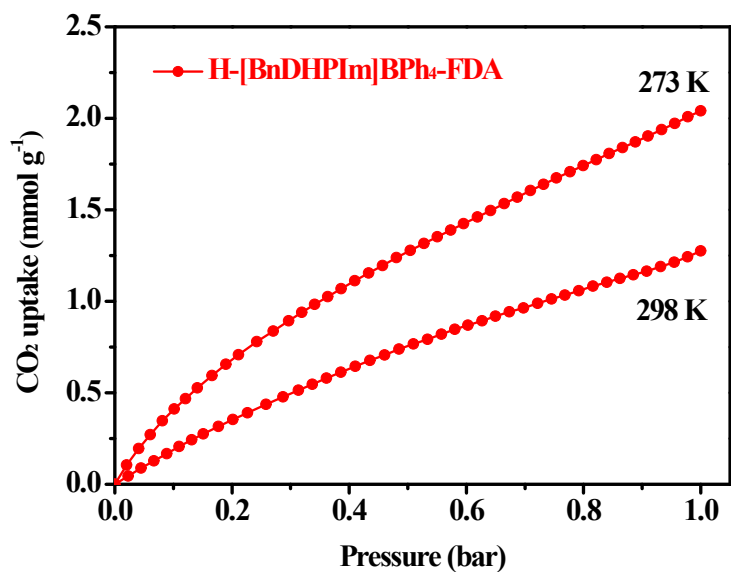
4. CO₂ adsorption

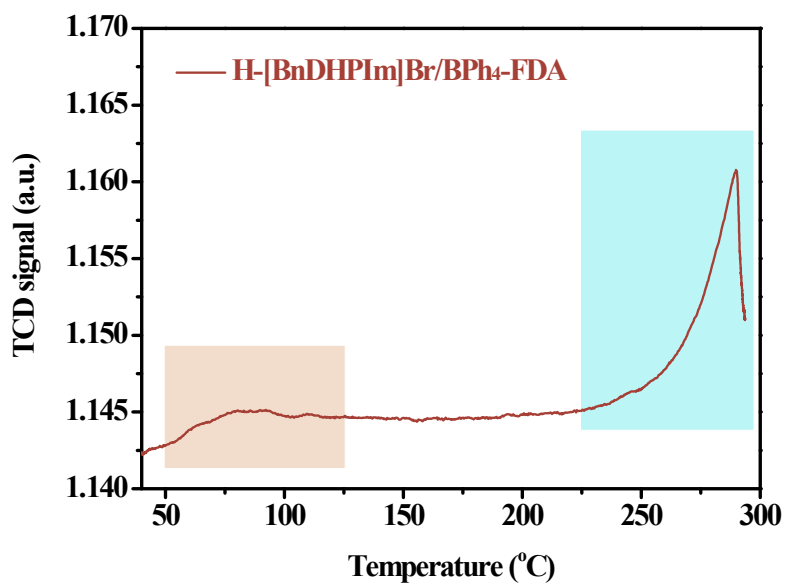**Figure S13** CO₂ adsorption isotherms of H-[BnDHPIm]BPh₄-FDA at 273 and 298 K.

Figure S14 CO₂-TPD profile of H-[BnDHPIm]Br/BPh₄-FDA.

Dual-site Langmuir–Freundlich isotherm model was used to describe the CO_2 adsorption, as follows:
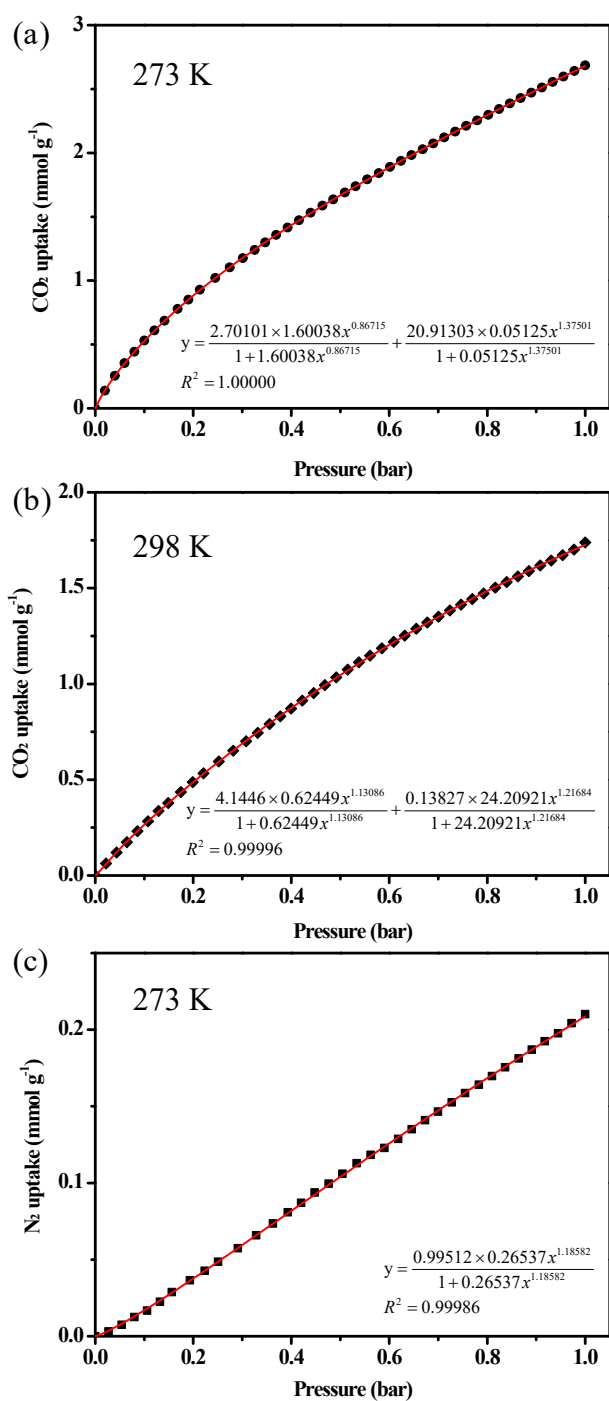
$$q = q_{i1} \times \frac{k_{i1} \times p^{\frac{1}{n_{i1}}}}{1 + k_{i1} \times p^{\frac{1}{n_{i1}}}} + q_{i2} \times \frac{k_{i2} \times p^{\frac{1}{n_{i2}}}}{1 + k_{i2} \times p^{\frac{1}{n_{i2}}}}$$

where q_{i1} (mmol g^{-1}), q_{i2} (mmol g^{-1}), k_{i1} (kPa^{-1}), k_{i2} (kPa^{-1}), n_{i1}, and n_{i2} are the parameters of the dual-site Langmuir–Freundlich isotherm model, p corresponds to equilibrium pressure.

Langmuir–Freundlich isotherm model was used to describe the N_2 adsorption, as follows:

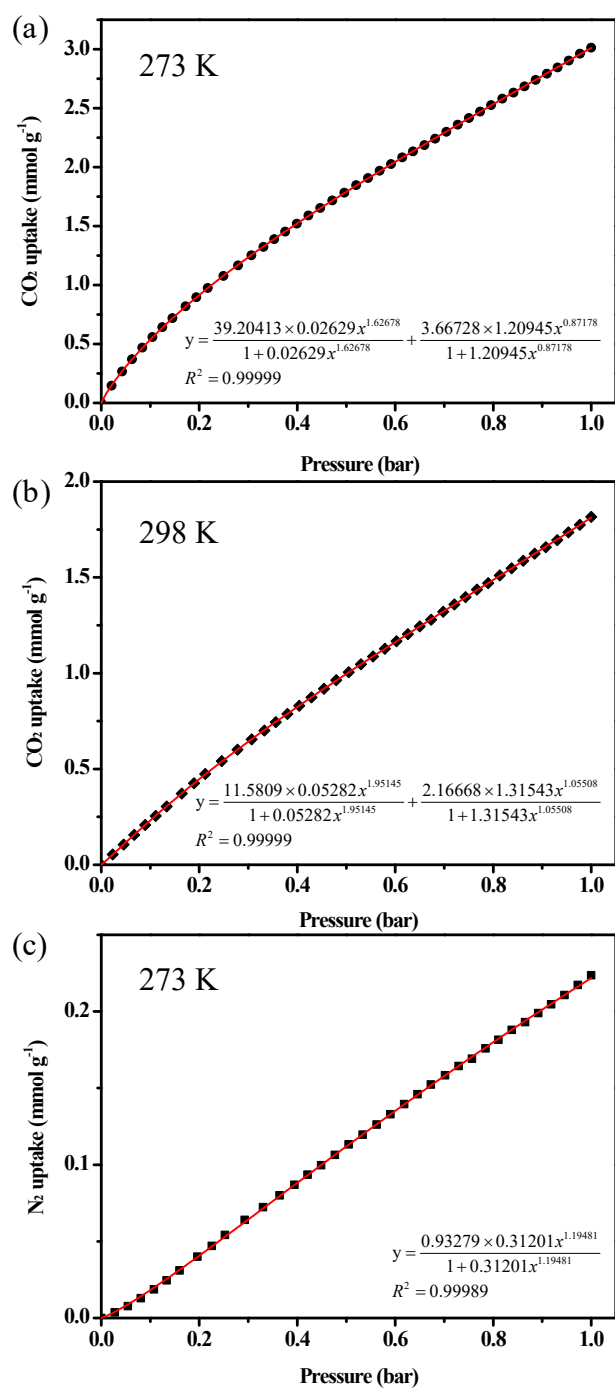$$q = q_i \times \frac{k_i \times p^{\frac{1}{n_i}}}{1 + k_i \times p^{\frac{1}{n_i}}}$$

where q_i (mmol g^{-1}), k_i (kPa^{-1}), and n_i are the parameters of the Langmuir–Freundlich isotherm model, p corresponds to equilibrium pressure.

(a)

273 K

$$y = \frac{2.70101 \times 1.60038 x^{0.86715}}{1 + 1.60038 x^{0.86715}} + \frac{20.91303 \times 0.05125 x^{1.37501}}{1 + 0.05125 x^{1.37501}}$$

$R^2 = 1.00000$

(b)

298 K

$$y = \frac{4.1446 \times 0.62449 x^{1.13086}}{1 + 0.62449 x^{1.13086}} + \frac{0.13827 \times 24.20921 x^{1.21684}}{1 + 24.20921 x^{1.21684}}$$

$R^2 = 0.99996$

(c)

273 K

$$y = \frac{0.99512 \times 0.26537 x^{1.18582}}{1 + 0.26537 x^{1.18582}}$$

$R^2 = 0.99986$

Figure S15 Non-linear curve fitting of (a) CO_2, 273 K, (b) CO_2, 298 K, and (c) N_2, 273 K adsorption isotherms of H-[BnEIm]Br/BPh$_4$-FDA.
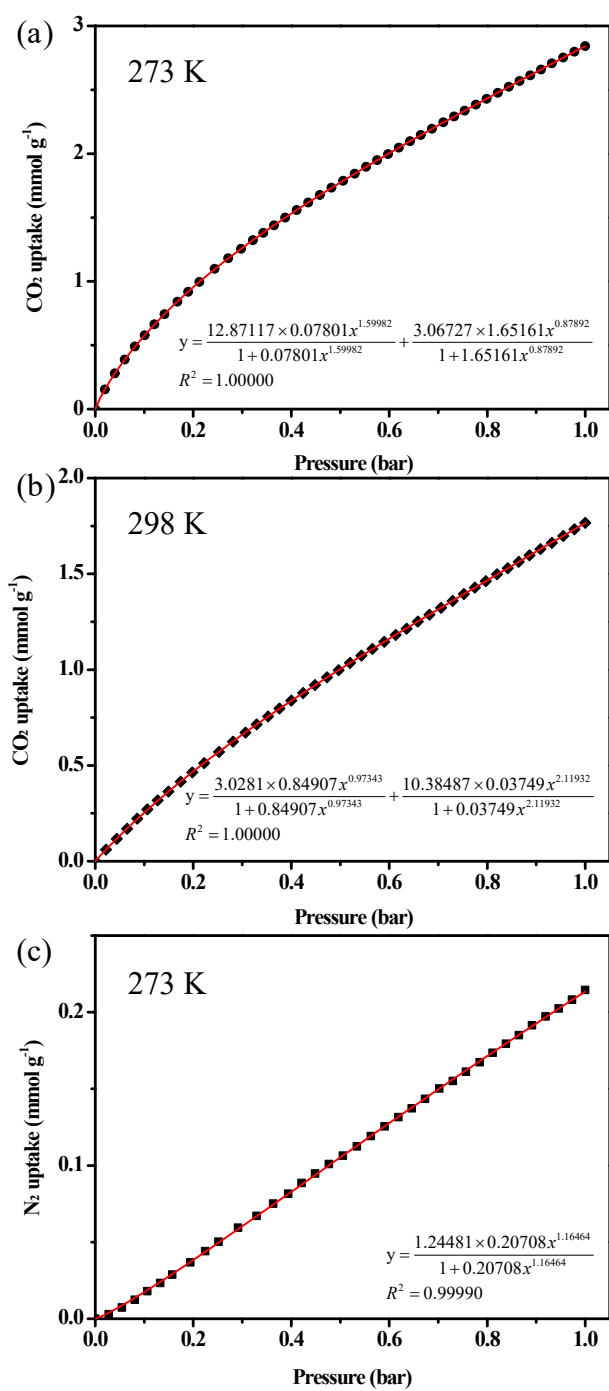
Figure S16 Non-linear curve fitting of (a) CO_2, 273 K, (b) CO_2, 298 K, and (c) N_2, 273 K adsorption isotherms of H-[BnHEIm]Br/BPh$_4$-FDA.

(a)

273 K

$$y = \frac{39.20413 \times 0.02629 x^{1.62678}}{1 + 0.02629 x^{1.62678}} + \frac{3.66728 \times 1.20945 x^{0.87178}}{1 + 1.20945 x^{0.87178}}$$

$R^2 = 0.99999$

(b)

298 K

$$y = \frac{11.5809 \times 0.05282 x^{1.95145}}{1 + 0.05282 x^{1.95145}} + \frac{2.16668 \times 1.31543 x^{1.05508}}{1 + 1.31543 x^{1.05508}}$$

$R^2 = 0.99999$

(c)

273 K

$$y = \frac{0.93279 \times 0.31201 x^{1.19481}}{1 + 0.31201 x^{1.19481}}$$

$R^2 = 0.99989$

Figure S17 Non-linear curve fitting of (a) CO_2, 273 K, (b) CO_2, 298 K, and (c) N_2, 273 K adsorption isotherms of H-[BnDHPIm]Br/BPh$_4$-FDA.
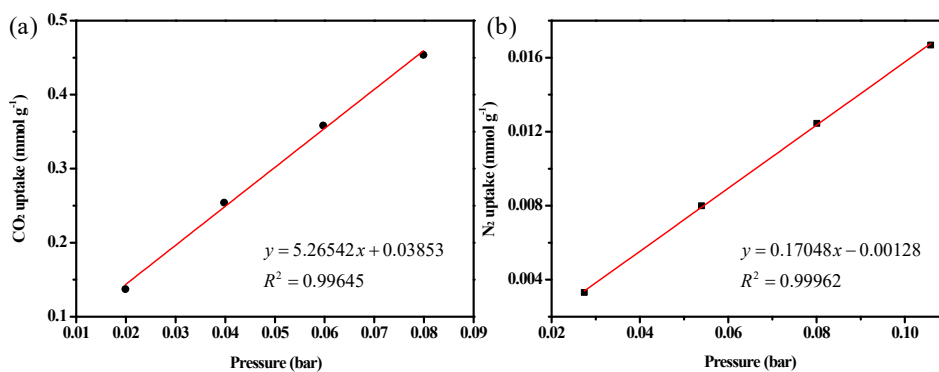
$$S(CO_2/N_2) = 30.9$$

Figure S18 CO_2/N_2 selectivity of H-[BnEIm]Br/BPh$_4$-FDA at 273 K calculated by using the Henry's law constants in the linear low-pressure range (< 0.11 bar).
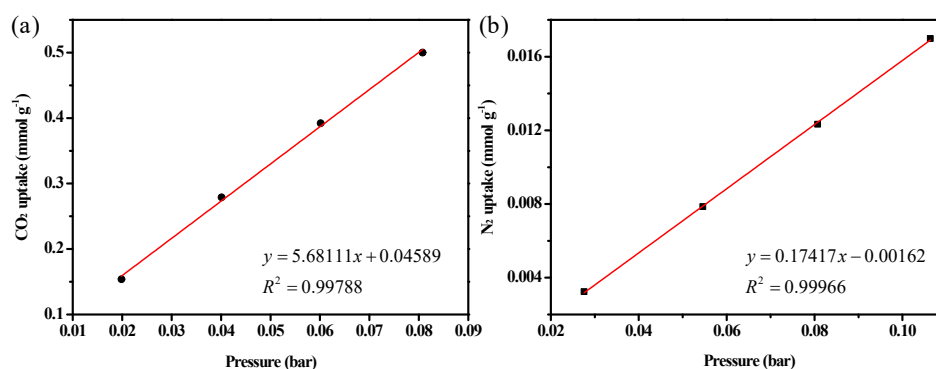
$$S(CO_2/N_2) = 32.6$$

Figure S19 CO_2/N_2 selectivity of H-[BnHEIm]Br/BPh$_4$-FDA at 273 K calculated by using the Henry's law constants in the linear low-pressure range (< 0.11 bar).
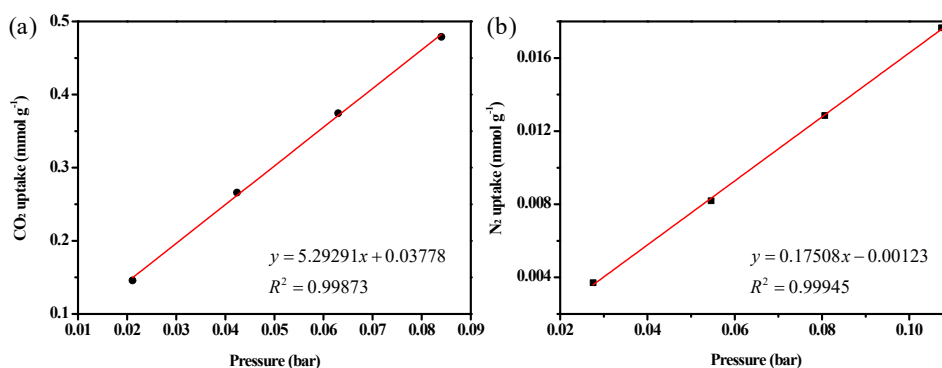
$$S(CO_2/N_2) = 30.2$$

Figure S20 CO_2/N_2 selectivity of H-[BnDHPIm]Br/BPh$_4$-FDA at 273 K calculated by using the Henry's law constants in the linear low-pressure range (< 0.11 bar).

Table S5 CO_2 uptakes and CO_2/N_2 selectivities of various hyper-crosslinked polymers (HCPs).

| HCP sample	CO_2 uptake[a] (mmol g^{-1})		CO_2/N_2 selectivity[b]		Reference
	273 K	298 K	Henry's law	IAST[c]	
HIP-Br-2	2.9	1.9	90	/	[4]
NHC-CAP-1(Zn^{2+})	2.80	1.72	100	/	[5]
CPIP-A-4	2.28	1.19	/	/	[6]
HPILs-Cl-2	1.80	1.00	7	37	[7]
IHCP-OH(1)	2.15	1.17	32	116	[8]
I$_{C2}$HCP-5b	3.05	/	86	336	[9]
HP-[BZPhIm]Cl-DCX-1	1.47	/	60	/	[10]
Py-HCP-Br	1.72	1.07	/	/	[11]
IHCP-2	2.87	1.79	14.1[d]	22.4[d]	[12]
PIPs-5	2.04	1.27	/	/	[13]
HPMBr0.5	1.74	0.93	/	/	[14]
Meso-PR-36	2.16	1.32	28	/	[15]
HCP1	2.64	1.57	15.3	23.6	[16]
Polymer 3	3.32	2.05	19.02	/	[17]
p-triptycene-72h-[ChCl][FeCl$_3$]$_2$	2.46	/	/	99	[18]
H-[BnDHPIm]Br/BPh$_4$-FDA	3.01	1.82	30.2	166	**This work**
H-[BnHEIm]Br/BPh$_4$-FDA	2.84	1.77	32.6	237	**This work**
H-[BnEIm]Br/BPh$_4$-FDA	2.68	1.74	30.9	177	**This work**

[a]CO_2 uptake at 273/298 K and 1 bar.

[b]CO_2/N_2 selectivity at 273 K.

[c]CO_2/N_2 selectivity at 273 K and 1 bar calculated by using the IAST model for the CO_2/N_2 (15% CO_2 + 85% N_2) mixture.

[d]CO_2/N_2 selectivity at 298 K.

## 5. CO_2 cycloaddition under ambient conditions

Optimization of the reaction conditions

To optimize the reaction conditions, the effects of amount of catalyst, reaction temperature, and reaction time on the fixation of CO_2 into styrene oxide to produce styrene carbonate under ambient conditions (1 bar CO_2) were investigated (Figures S21–S23). As shown in Figure S21, the yield of styrene carbonate increased from 66.0 to 76.2 % as the amount of H-[BnDHPIm]Br/BPh$_4$-FDA increased from 2 to 5 wt%. However, when further increasing the amount to 6 wt%, the yield slightly decreased to 74.1%. This might be because, with the increase of the amount of heterogeneous H-[BnDHPIm]Br/BPh$_4$-FDA, in addition to the increase of the number of active centers, the mass transfer resistance was also increased. Furthermore, the yield of styrene carbonate increased gradually with an increase in reaction temperature or reaction time (Figures S22 and S23). Regardless of how to alter the amount of H-[BnDHPIm]Br/BPh$_4$-FDA, reaction temperature, or reaction time, the selectivity of styrene carbonate was always > 99 %. The reaction was not completely transformed because a small amount of the reactant styrene oxide condensed on the inner wall of the reaction Schlenk tube (Figure S24). Overall, under the optimized reaction conditions (1 bar CO_2, 4 wt% H-[BnDHPIm]Br/BPh$_4$-FDA, T = 80 ºC, t = 15 h), a remarkable catalytic activity with 94.2 % yield and > 99 % selectivity of styrene carbonate was achieved.
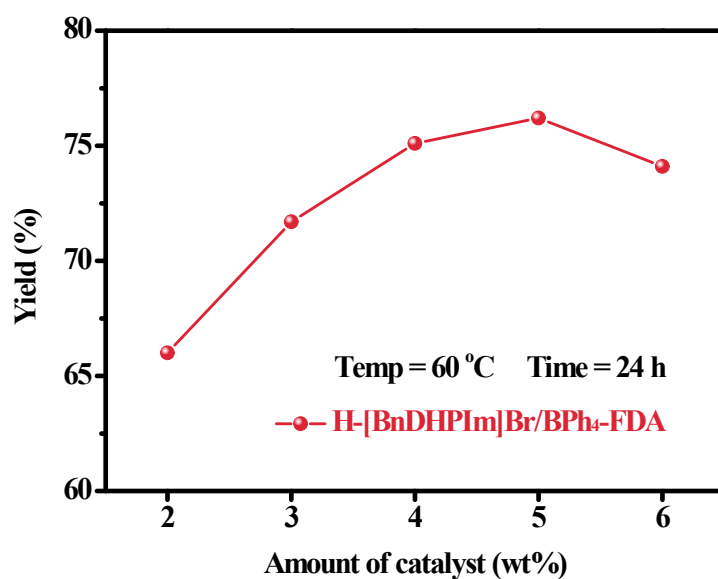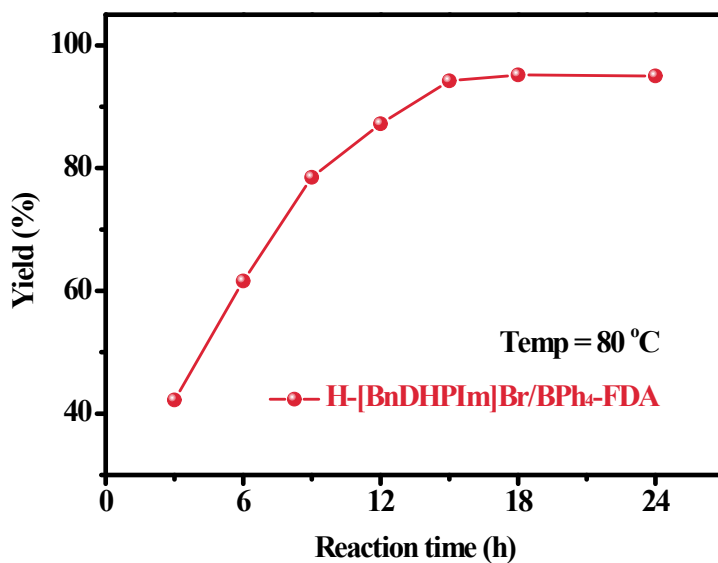
Figure S21 Effect of amount of catalyst H-[BnDHPIm]Br/BPh$_4$-FDA. Reaction conditions: 12.5 mmol styrene oxide, 1 bar (balloon) CO_2, 2 mol% TBABr, 60 ºC, 24 h.
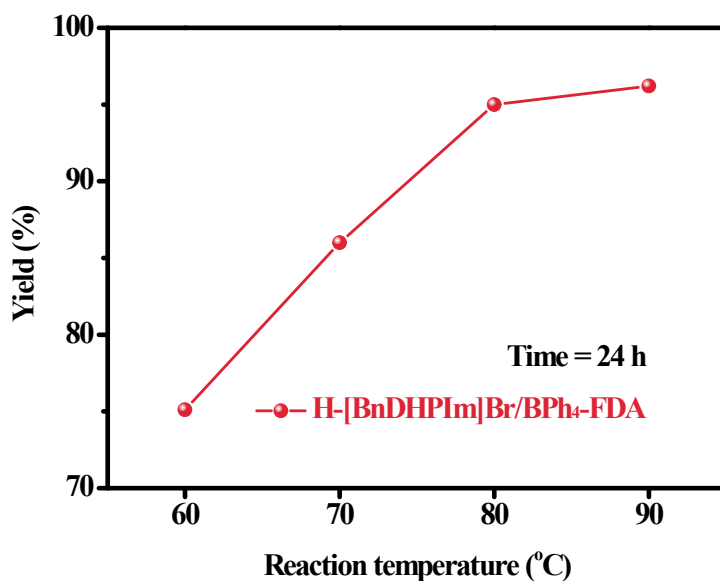
Figure S22 Effect of reaction temperature. Reaction conditions: 12.5 mmol styrene oxide, 1 bar (balloon) CO_2, 4 wt% H-[BnDHPIm]Br/BPh$_4$-FDA, 2 mol% TBABr, 24 h.

Figure S23 Effect of reaction time. Reaction conditions: 12.5 mmol styrene oxide, 1 bar (balloon) CO_2, 4 wt% H-[BnDHPIm]Br/BPh$_4$-FDA, 2 mol% TBABr, 80 °C.
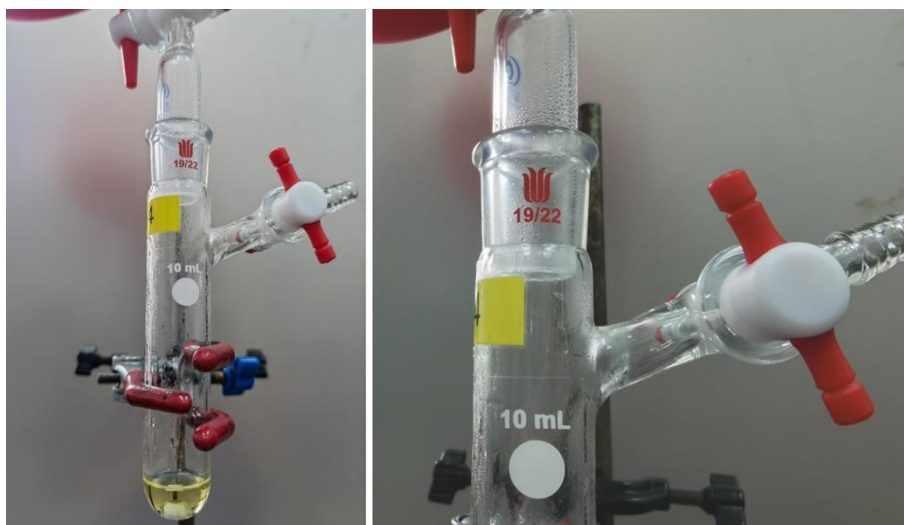
Figure S24 Condensation phenomenon of styrene oxide in the CO_2 cycloaddition reaction at ambient pressure. Reaction conditions: 12.5 mmol styrene oxide, 1 bar (balloon) CO_2, 2.5 mol% TBABr, 80 °C, 24 h.

Table S6 Comparison of the catalytic performance of H-[BnDHPIm]Br/BPh$_4$-FDA with the previously reported efficient catalytic system in the cycloaddition of CO$_2$ with styrene oxide.

Entry	Catalyst	Co-catalyst	P (bar)	T (°C)	t (h)	Yield (%)	TOF[a] (h^{-1})	Productivity[b] (g g^{-1} h^{-1})	Reference
1	H-[BnDHPIm]Br/BPh$_4$-FDA	TBABr (2 mol%)	1	80	15	94.2	10.9	2.15	**This work**
2	HCIP-4	TBABr (0.3 mol%)	10	120	6	87	–	5.95	[19]
3	HPILs-Cl-2	TBABr (25 mol%)	1	70	9	88	–	3.21	[7]
4	DHI-CSU-3-Br	TBABr (17 mol%)	1	70	8	79	–	1.62	[20]
5	IHCP-OH(1)	–	30	135	2	94	1410	115.73	[8]
6	I$_{C2}$HCP-5b	–	30[c]	120	32	87	136	–	[9]
7	Py-HCP-Br	–	20	120	8	86	–	1.52	[11]
8	NHC-CAP-1(Zn^{2+})	–	20	100	3	81	–	73.6	[5]
9	HP-[BZPhIm]Cl-DCX-1	–	10	120	10	81.2	–	2.22	[10]
10	PIPs-5	–	10	120	8	99	20.6	4.06	[13]
11	HPMBr0.5	–	1	80	36	94.7	3.8	1.44	[14]
12	[MgCo$_2$O$_4$]-[Cl$^-$]	TBAI[d] (3 mol%)	1	100	12	91.2	0.60	1.38	[21]
13	Co(III)−P5COP	TBABr (10 mol%)	1	80	36	99	–	1.13	[22]
14	Zr-AZDA	TBABr (2 mol%)	1	80	24	92.6	3.86	–	[23]
15	CuBDC/CMC	TBABr (2 mol%)	1	80	17	91.5	10.8	0.69	[24]
16	10.26 wt% PMo$_{12}$@Zr-Fc	TBABr (2 mol%)	1	80	8	86.77	75.1	–	[25]
17[e]	USTC-9(Fe)	TBABr (31 mol%)	1	70	48	73.2	–	0.025	[26]
18	Ir$_1$–WO$_3$	TBABr (3.1 mol%)	1	40	15	98	–	1.07	[27]

[a]TOF = [mmol (product)]/[mmol (active centers) × reaction time]; Entries 1–11, based on IL centers; Entries 12–18, based on metal centers.

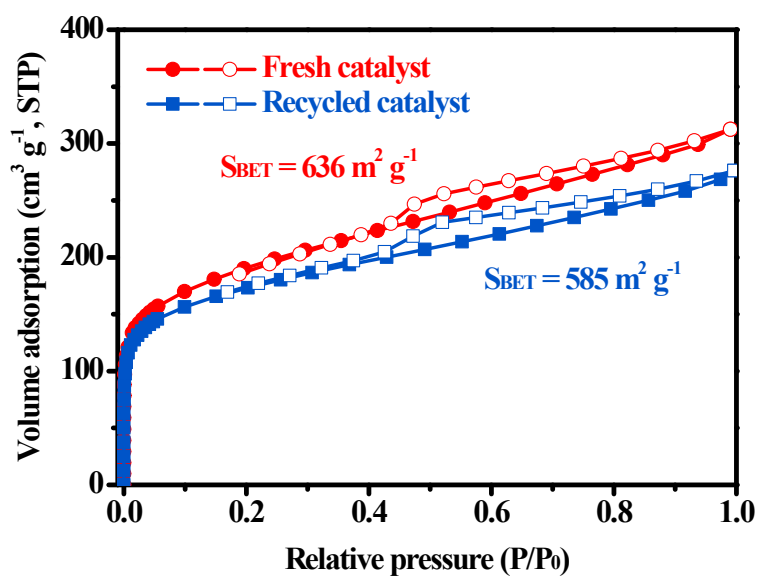[b]Productivity = [g (product)]/[g (catalyst) × reaction time].

[c]15 % CO$_2$ + 85 % N$_2$.
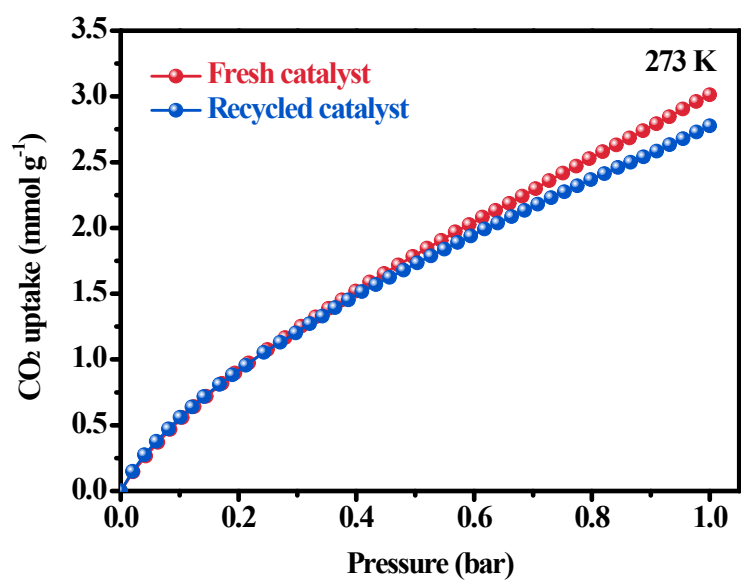
[d]TBAI: tetrabutylammonium iodide.

[e]3 mL acetonitrile.
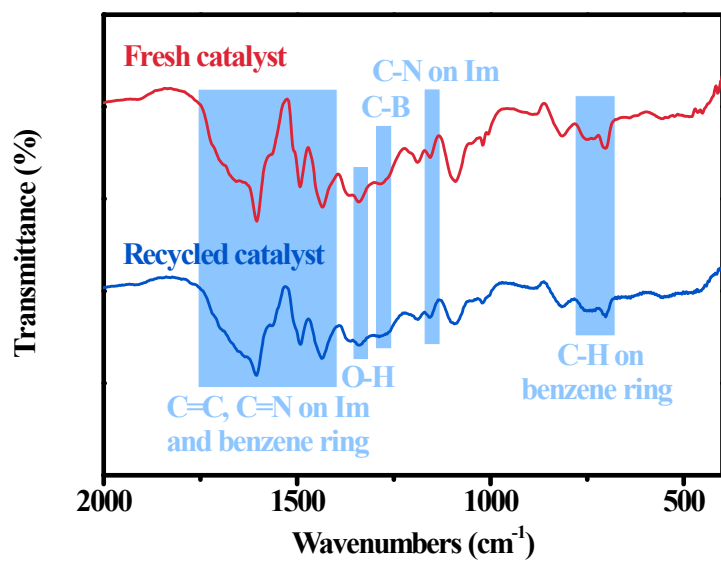
Figure S25 FT-IR spectra of fresh and recycled catalyst H-[BnDHPIm]Br/BPh$_4$-FDA.

Figure S26 N$_2$ adsorption-desorption isotherms of fresh and recycled catalyst H-[BnDHPIm]Br/BPh$_4$-FDA.
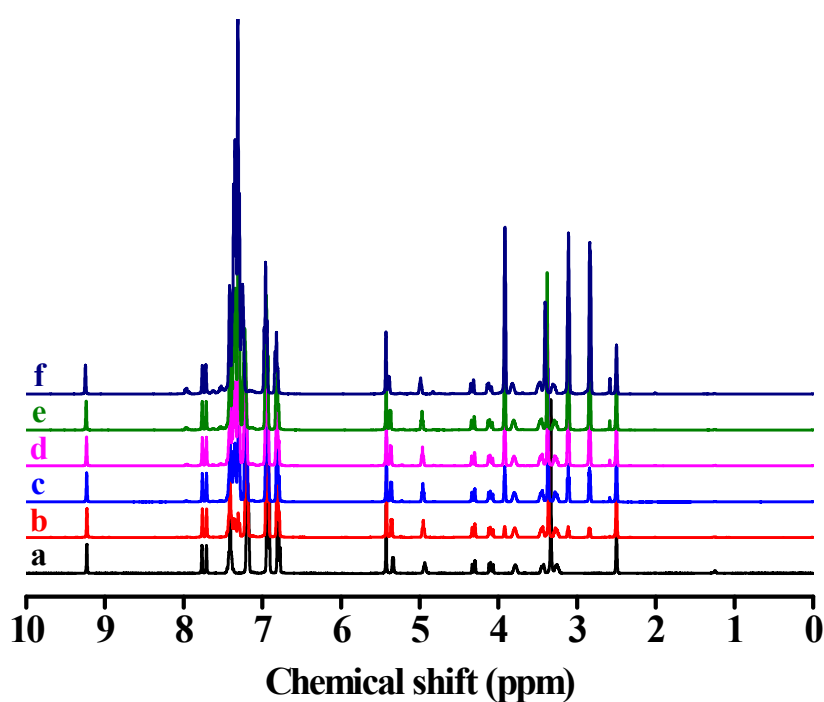
Figure S27 CO_2 adsorption isotherms of fresh and recycled catalyst H-[BnDHPIm]Br/BPh$_4$-FDA at 273 K.

6. Effect of hydroxyl on CO₂ capture and conversion

Table S7 The bond length (Å) of the optimized structures.

Bond length	[BnDHPIm]$^+$	Complex of [BnDHPIm]$^+$ with CO_2
O1—H1	0.97767	0.97814
O2—H2	0.97170	0.97437
C—H3	1.07319	1.07333

Figure S28 ^{1}H-NMR titration of [BnDHPIm]BPh₄ in DMSO-d₆ with different amounts of styrene oxide (SO). a) [BnDHPIm]BPh₄, b) [BnDHPIm]BPh₄/SO = 1 : 0.5, c) 1 : 1, d) 1 : 2.5, e) 1 :5, f) 1:10 (molar ratio), respectively.
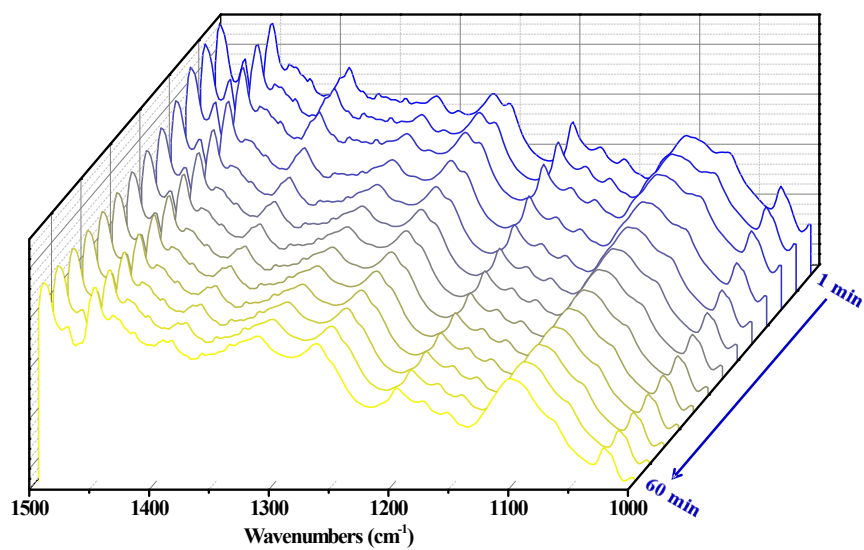
Figure S29 *In-situ* FT-IR spectra of H-[BnDHPIm]Br/BPh$_4$-FDA with styrene oxide adsorbed at 80 ºC for 60 min.

7. NMR spectra of the IL monomers

¹H-NMR (CDCl₃)

¹H-NMR (DMSO-d₆)

^{13}C-NMR (DMSO-d$_6$)

164.58
164.09
163.60
163.11

136.63
136.01
125.83
125.80
125.78
125.75
124.03
122.42
122.00

44.59
36.14
15.57

190 170 150 130 110 90 80 70 60 50 40 30 20 10 0
f1 (ppm)

^{1}H-NMR (DMSO-d$_6$)

9.50

7.87
7.47
7.45
7.43
7.42
7.40
7.37
7.36

5.47

4.25
4.23
4.21
4.20

1.44
1.42
1.40

1.00
2.03
5.15
2.05
2.12
3.12

.0   9.5   8.5   7.5   6.5   5.5   4.5   3.5   2.5   1.5   0.5
f1 (ppm)
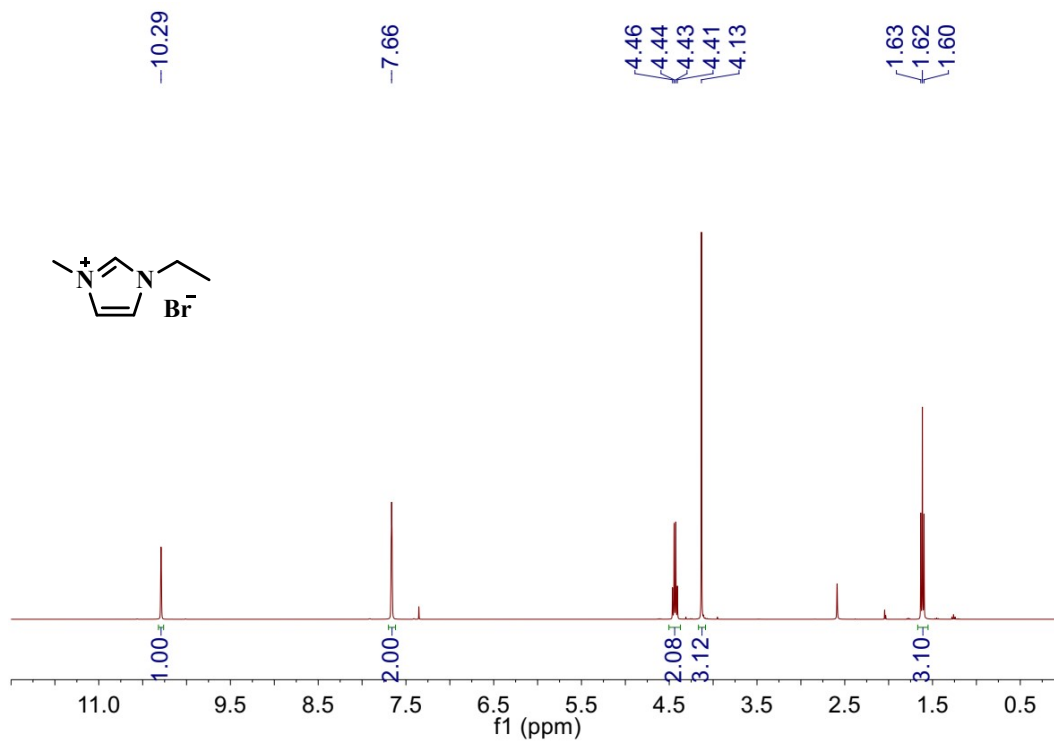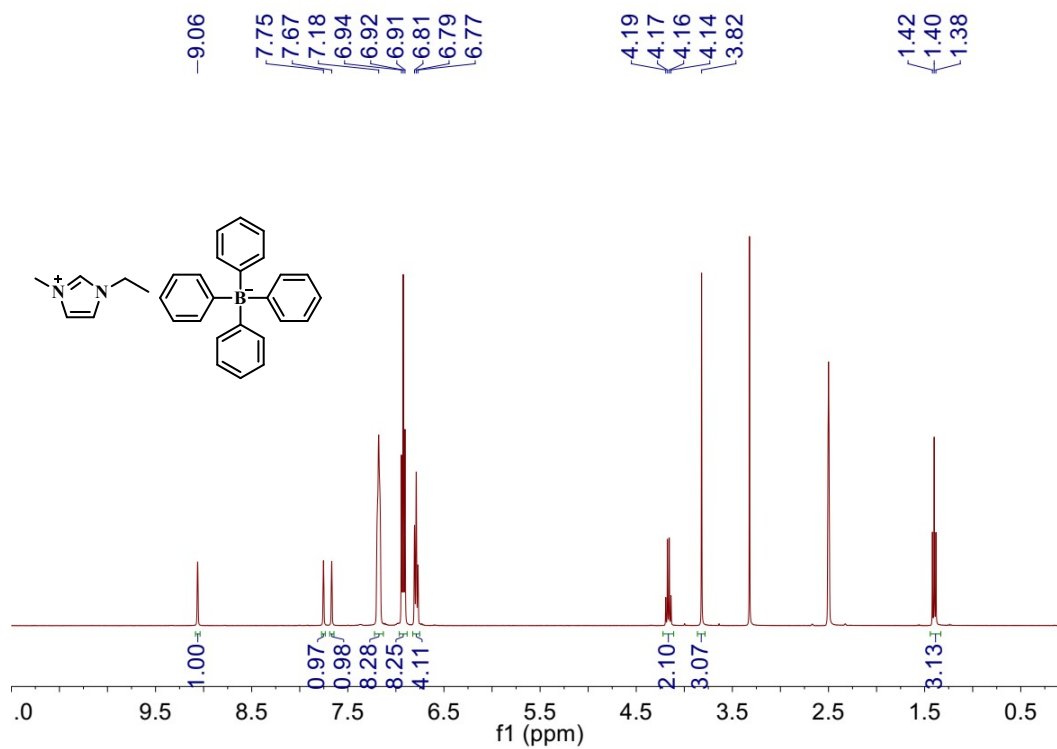
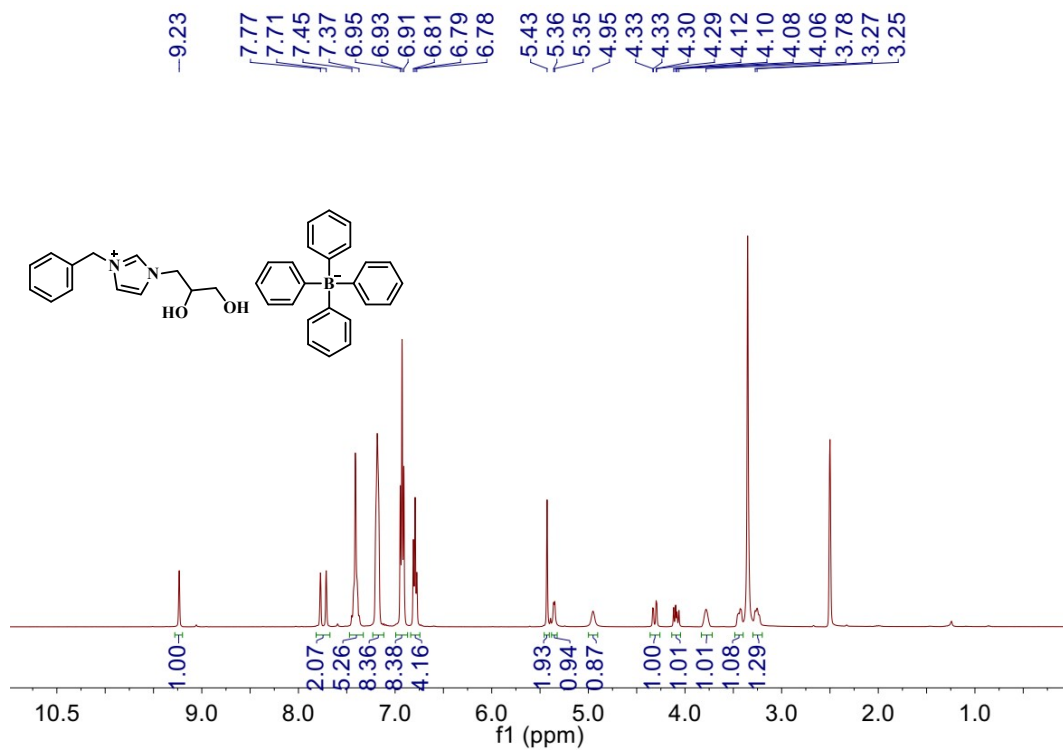# ¹H-NMR (DMSO-d₆)
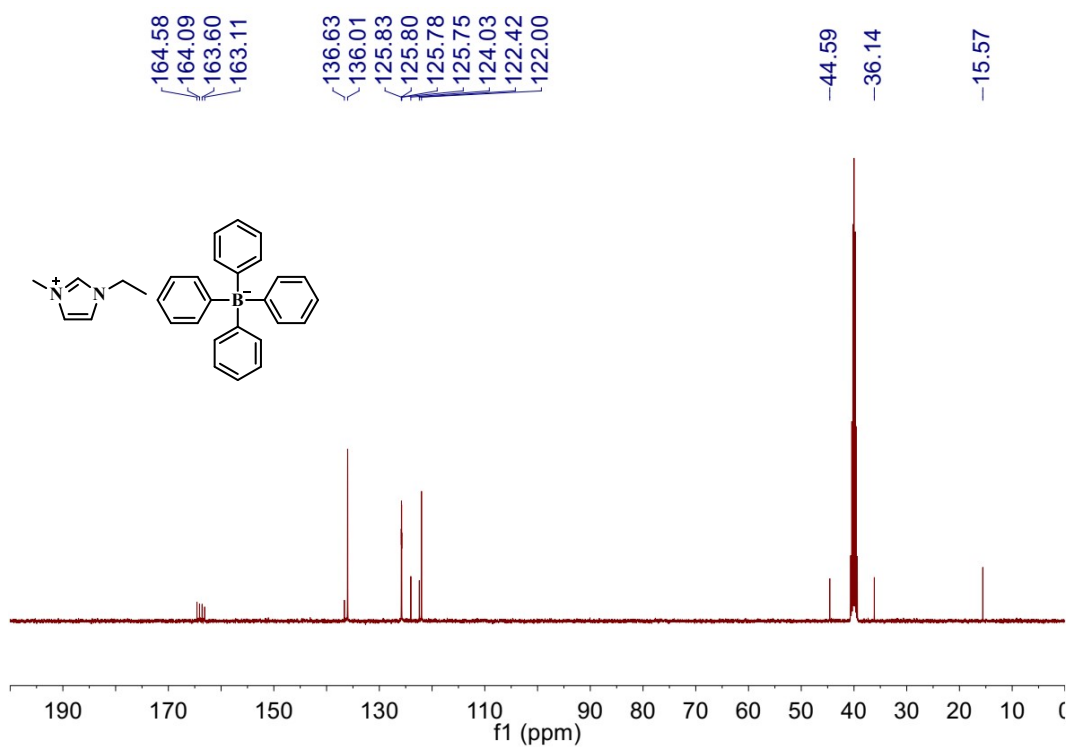
¹H-NMR (DMSO-d$_6$)
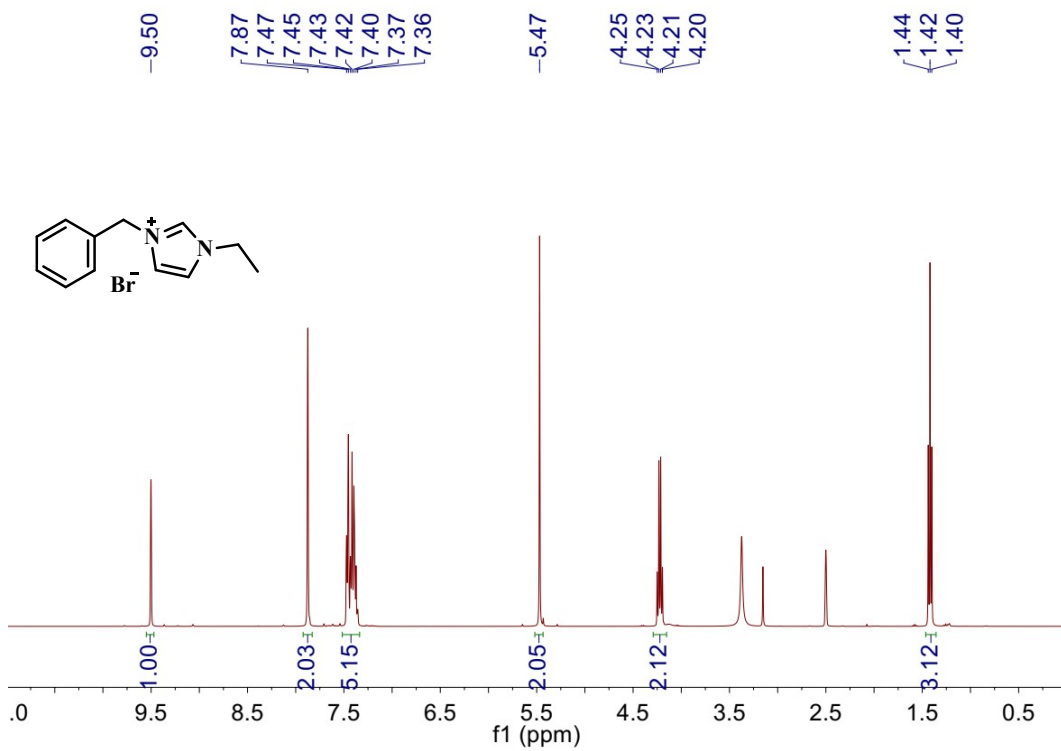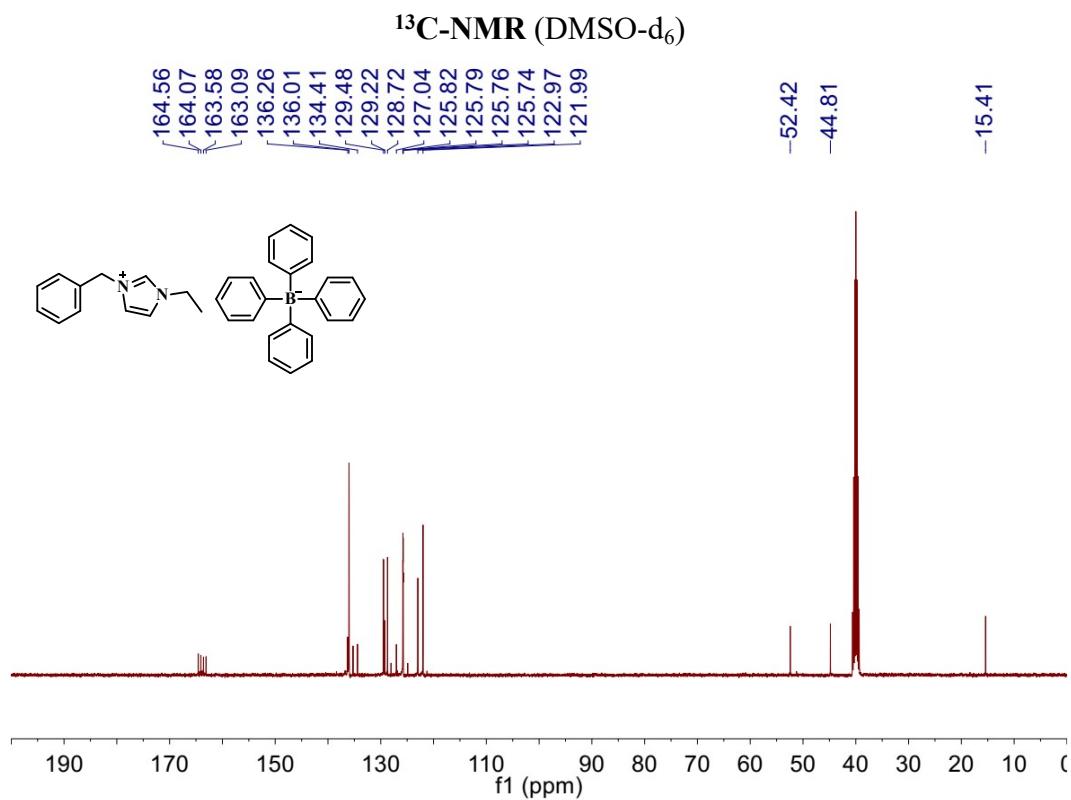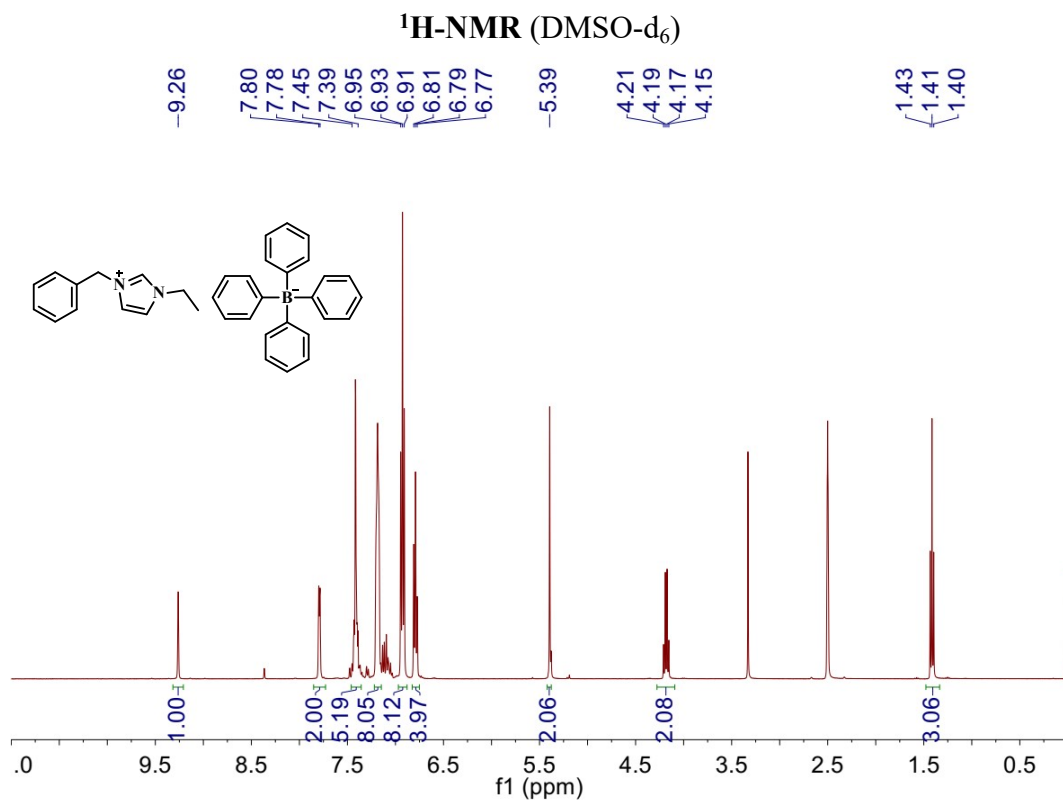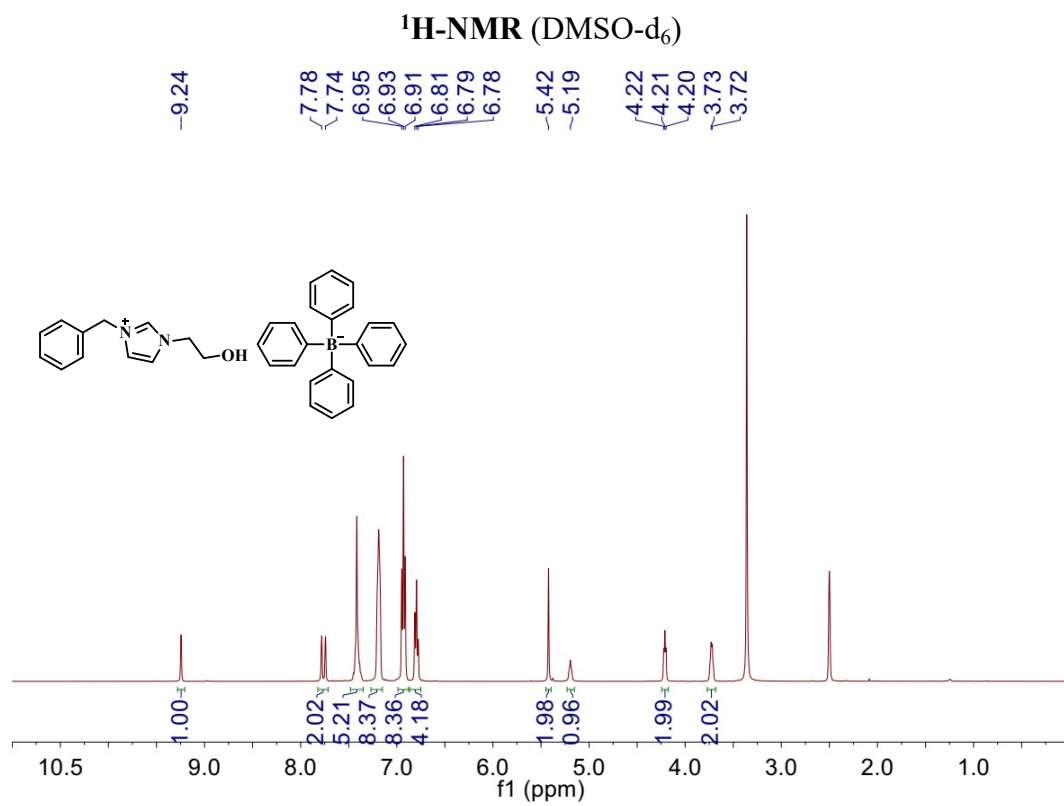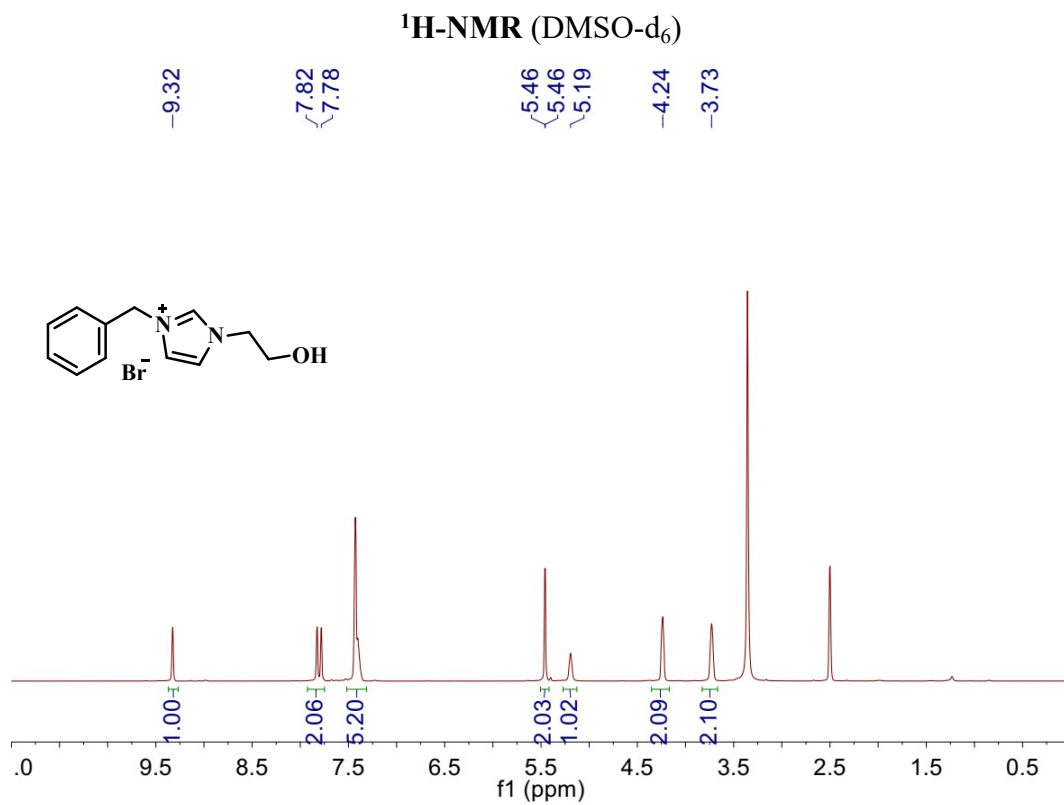
¹³C-NMR (DMSO-d₆)

¹³C-NMR (DMSO-d$_6$)

¹H-NMR (DMSO-d₆)

¹H-NMR (DMSO-d₆)

^{13}C-NMR (DMSO-d$_6$)

164.55
164.06
163.57
163.08
136.94
135.99
135.34
129.46
129.20
128.68
125.80
125.78
125.75
125.73
123.63
122.74
121.98
59.65
52.30
52.25

190 170 150 130 110 90 80 70 60 50 40 30 20 10 0
f1 (ppm)

^{1}H-NMR (DMSO-d$_6$)

7.56
7.12
6.86
4.81
4.09
4.08
4.06
4.05
3.89
3.87
3.86
3.84
3.68
3.67
3.36
3.34
3.33
3.32
3.23
3.22
3.21

1.00
1.04
1.10
2.53
1.02
1.02
1.03
1.02
1.63

9.5 8.5 7.5 6.5 5.5 4.5 3.5 2.5 1.5 0.5
f1 (ppm)

^{1}H-NMR (DMSO-d$_6$)

^{1}H-NMR (DMSO-d$_6$)

^{13}C-NMR (DMSO-d$_6$)

164.55
164.06
163.57
163.08
137.21
136.00
135.36
129.46
129.19
128.63
125.81
125.78
125.75
125.73
124.18
122.51
121.98

69.96
63.22
52.80
52.29

190 170 150 130 110 90 80 70 60 50 40 30 20 10 0
f1 (ppm)

8. NMR spectra of the cyclic carbonate products

^{1}H-NMR (CDCl$_3$)
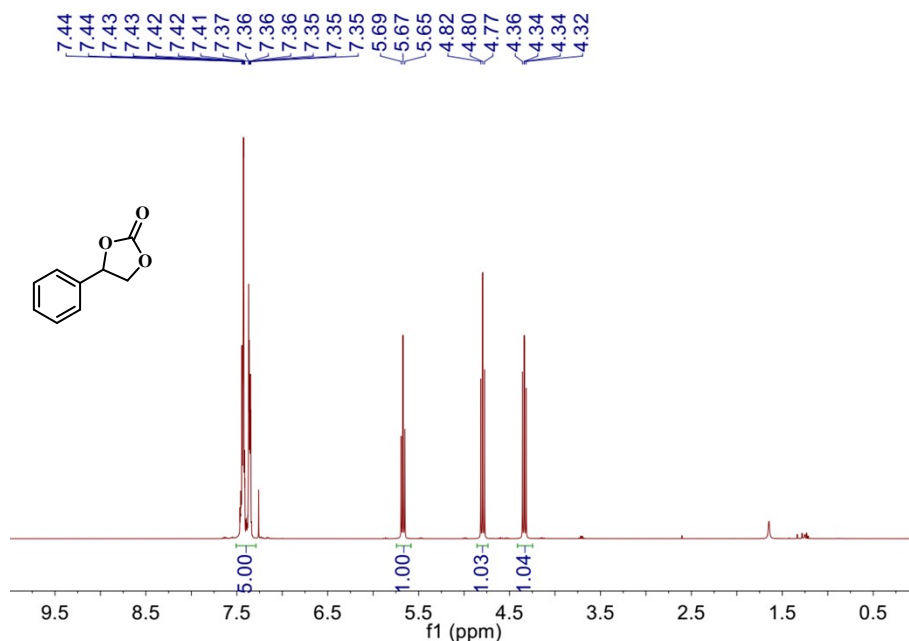
^{1}H NMR (400 MHz, CDCl$_3$, TMS) δ (ppm): 7.44–7.35 (m, 5H), 5.67 (t, J = 8.0 Hz, 1H), 4.80 (t, J = 8.4 Hz, 1H), 4.34 (dd, J = 8.4 Hz, J = 8.0 Hz, 1H).

^{13}C-NMR (CDCl$_3$)
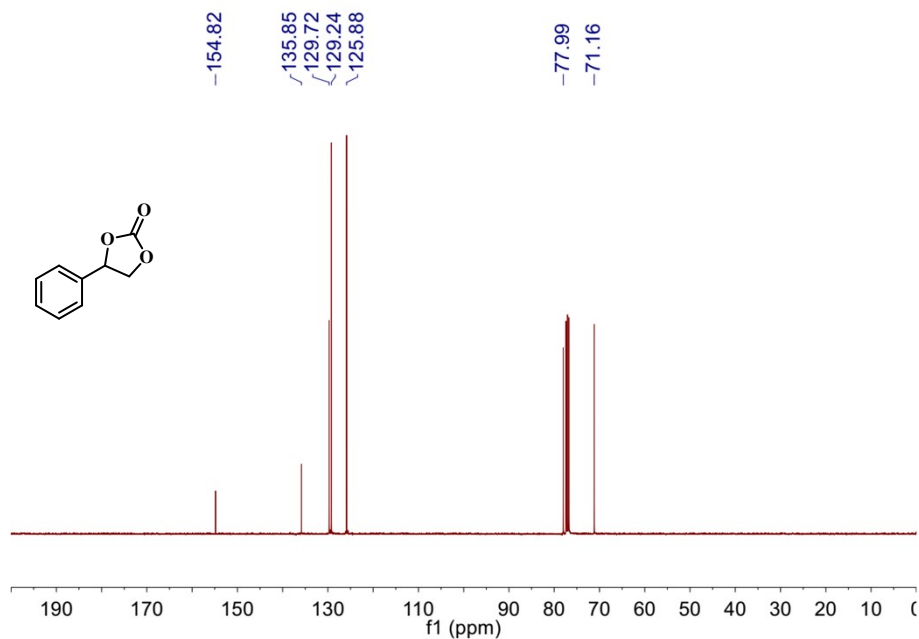
^{13}C NMR (100 MHz, CDCl$_3$, TMS) δ (ppm): 154.82, 135.85, 129.72, 129.24, 125.88, 77.99, 71.16.

¹H-NMR (CDCl₃)
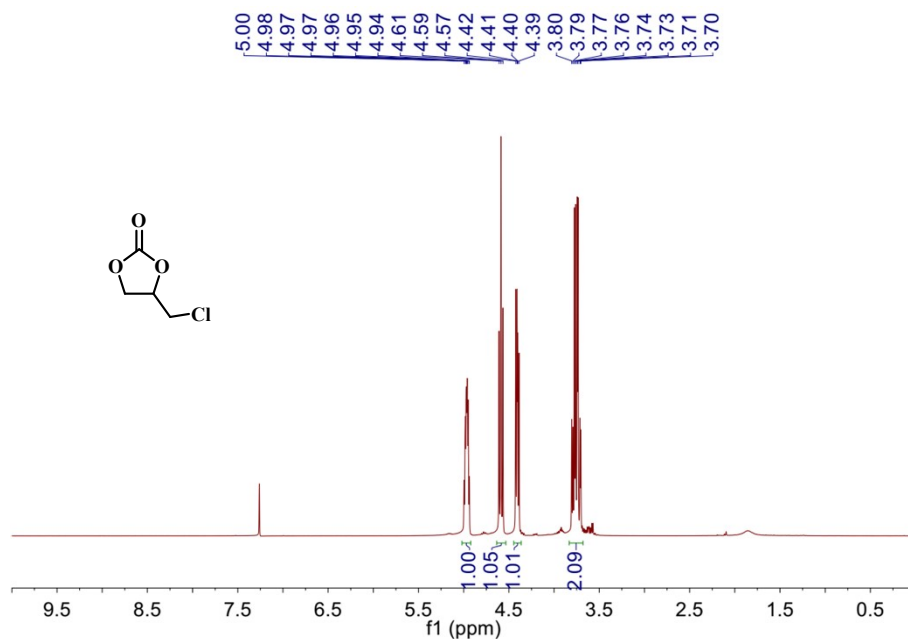
¹H NMR (400 MHz, CDCl₃, TMS) δ (ppm): 5.00–4.94 (m, 1H), 4.59 (t, J = 8.4 Hz, 1H), 4.42–4.39 (m, 1H), 3.80–3.70 (m, 2H).

¹³C-NMR (CDCl₃)
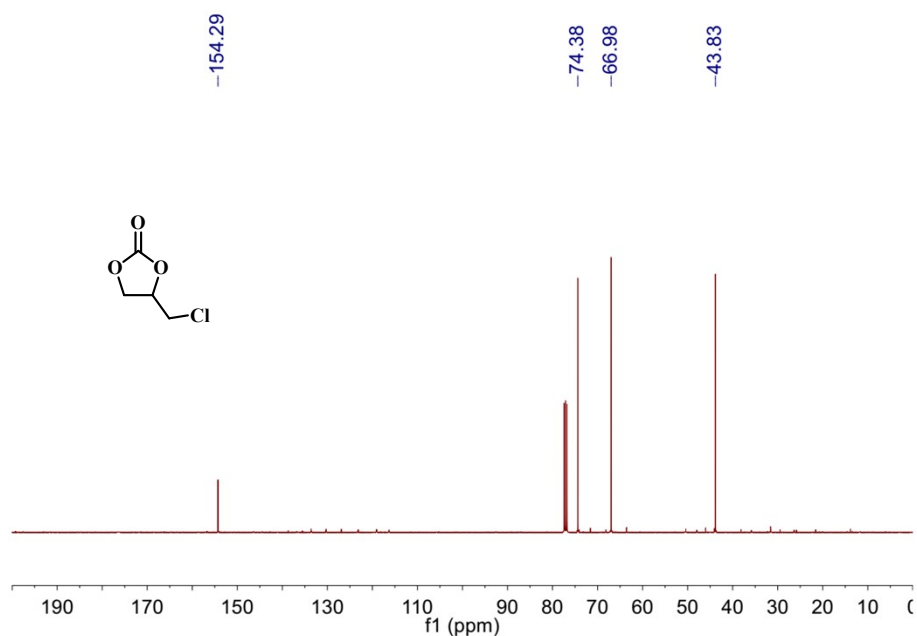
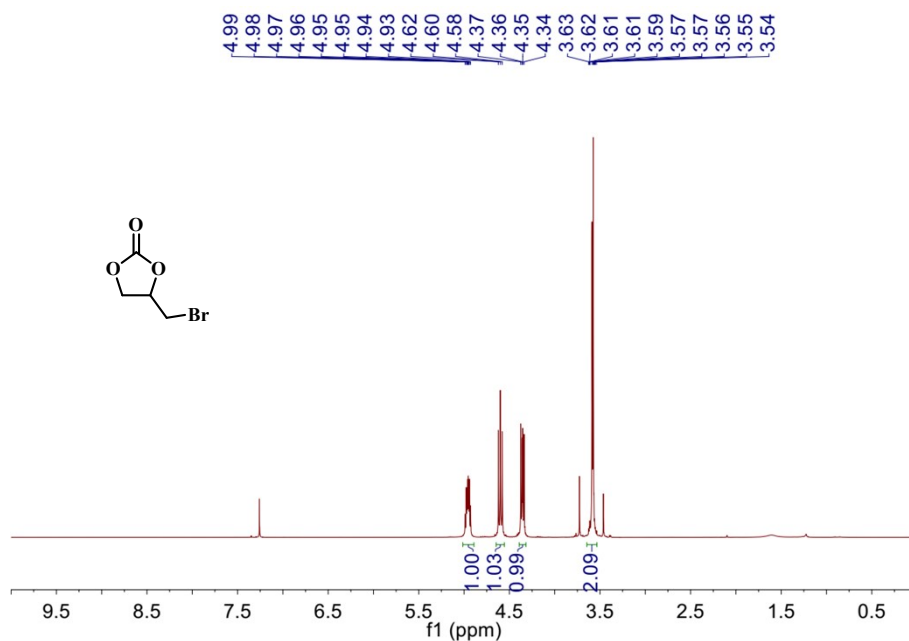
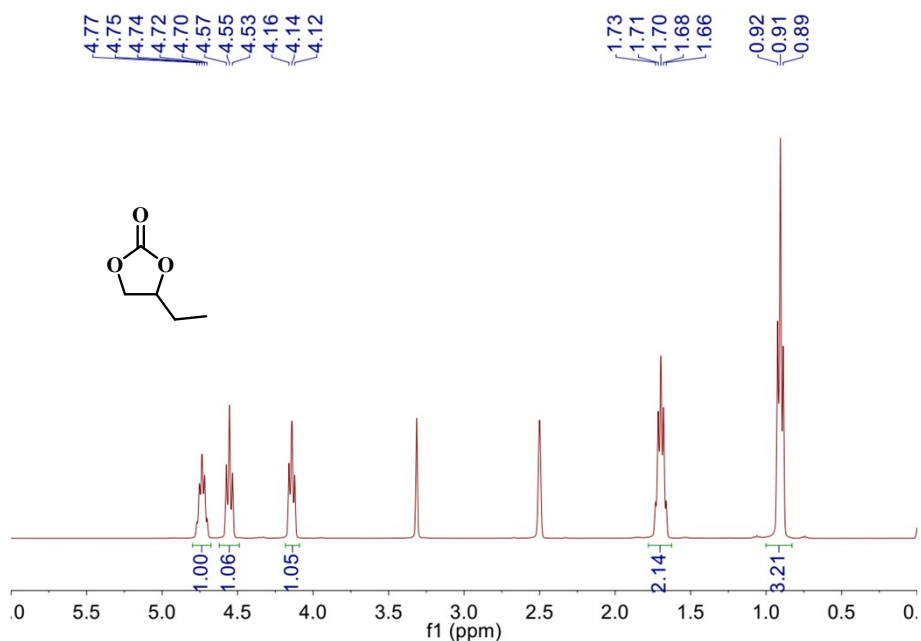¹³C NMR (100 MHz, CDCl₃, TMS) δ (ppm): 154.29, 74.38, 66.98, 43.83.

^{1}H-NMR (CDCl$_3$)

^{1}H NMR (400 MHz, CDCl$_3$, TMS) δ (ppm): 4.99–4.93 (m, 1H), 4.60 (t, J = 8.4 Hz, 1H), 4.37–4.34 (m, 1H), 3.63–3.54 (m, 2H).
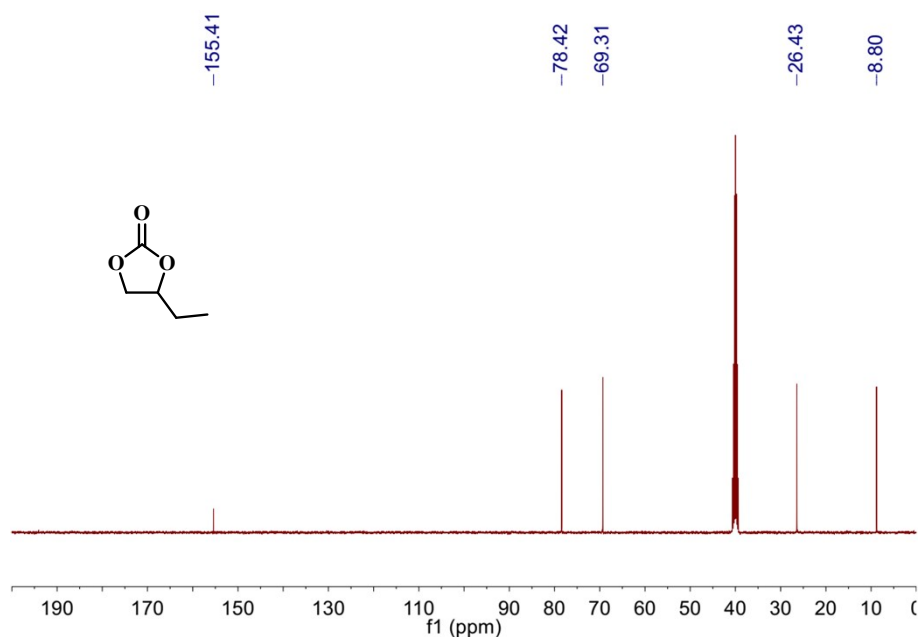
^{13}C-NMR (CDCl$_3$)
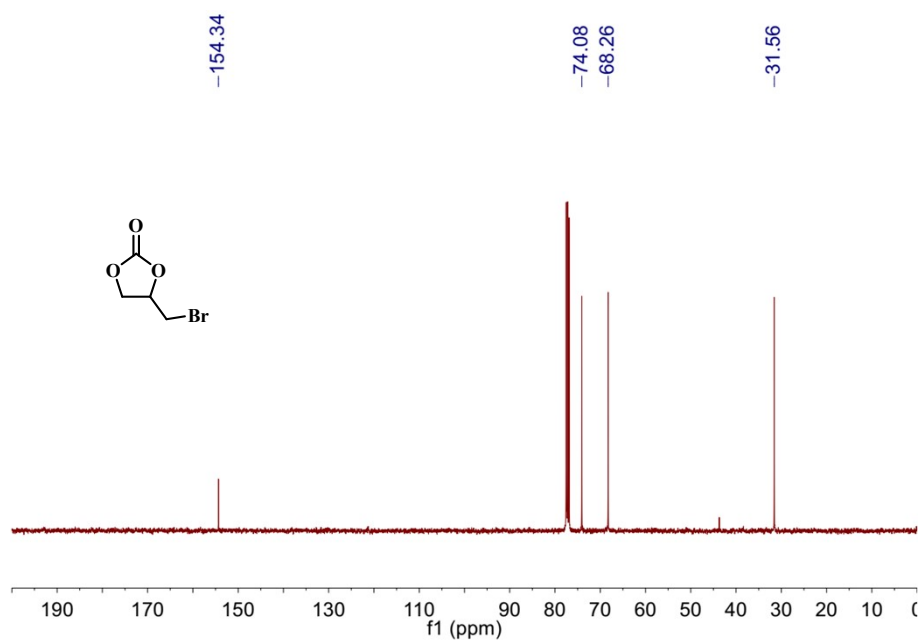
^{13}C NMR (100 MHz, CDCl$_3$, TMS) δ (ppm): 154.34, 74.08, 68.26, 31.56.

¹H-NMR (DMSO-d₆)

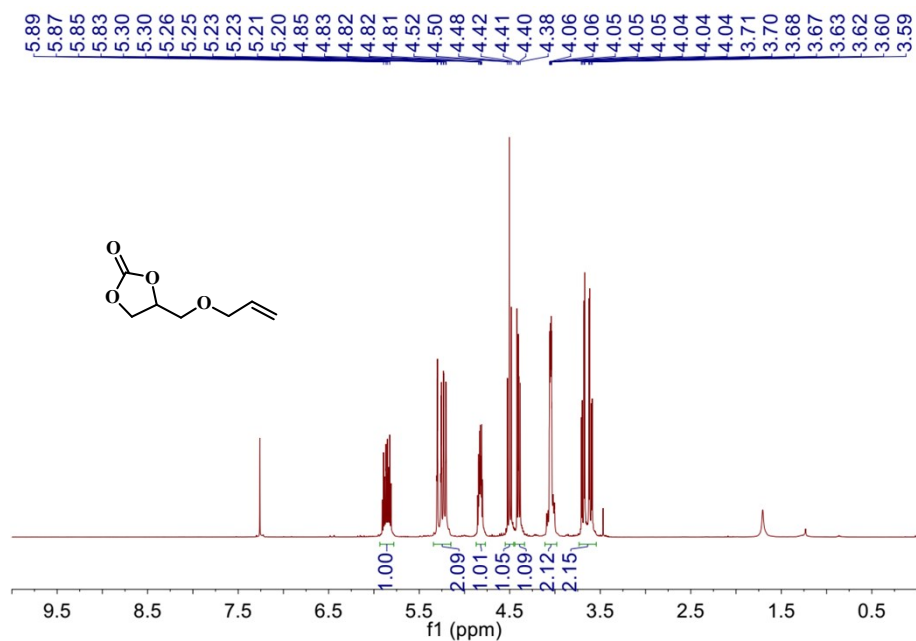¹H NMR (400 MHz, DMSO-d₆, TMS) δ (ppm): 4.77–4.70 (m, 1H), 4.55 (t, J = 8.0 Hz, 1H), 4.14 (t, J = 7.6 Hz, 1H), 1.73–1.66 (m, 2H), 0.91 (t, J = 7.4 Hz, 3H).
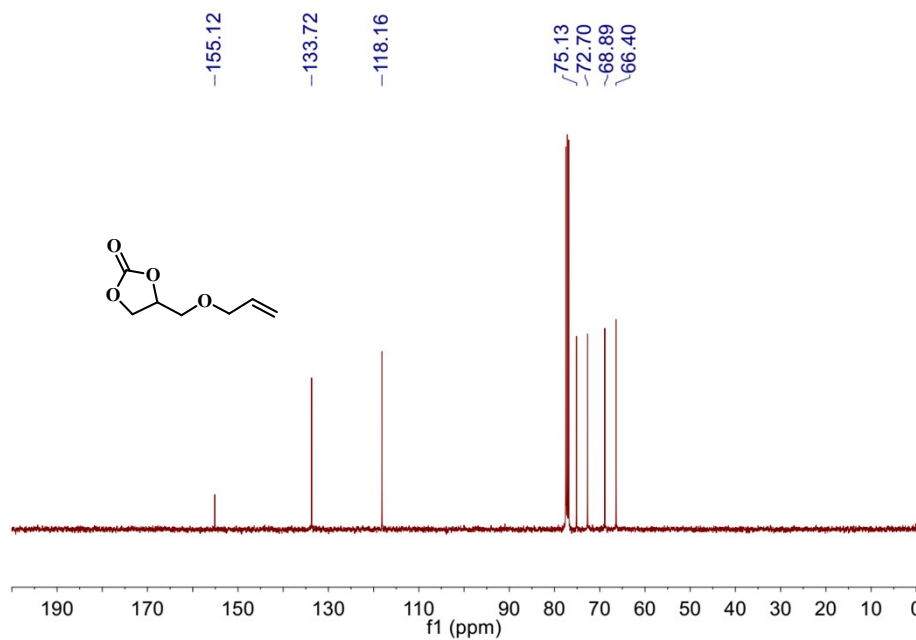
¹³C-NMR (DMSO-d₆)

¹³C NMR (100 MHz, DMSO-d₆, TMS) δ (ppm): 155.41, 78.42, 69.31, 26.43, 8.80.
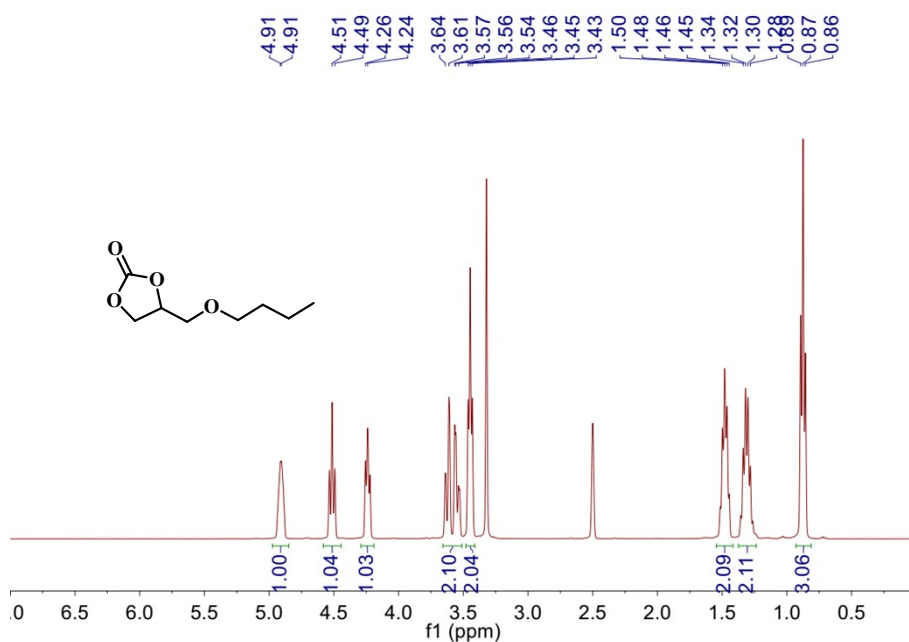
¹H-NMR (CDCl₃)

¹H NMR (400 MHz, CDCl₃, TMS) δ (ppm): 5.91–5.81 (m, 1H), 5.31–5.20 (m, 2H), 4.85–4.80 (m, 1H), 4.50 (t, J = 8.4 Hz, 1H), 4.42–4.38 (m, 1H), 4.06–4.04 (m, 2H), 3.71–3.59 (m, 2H).
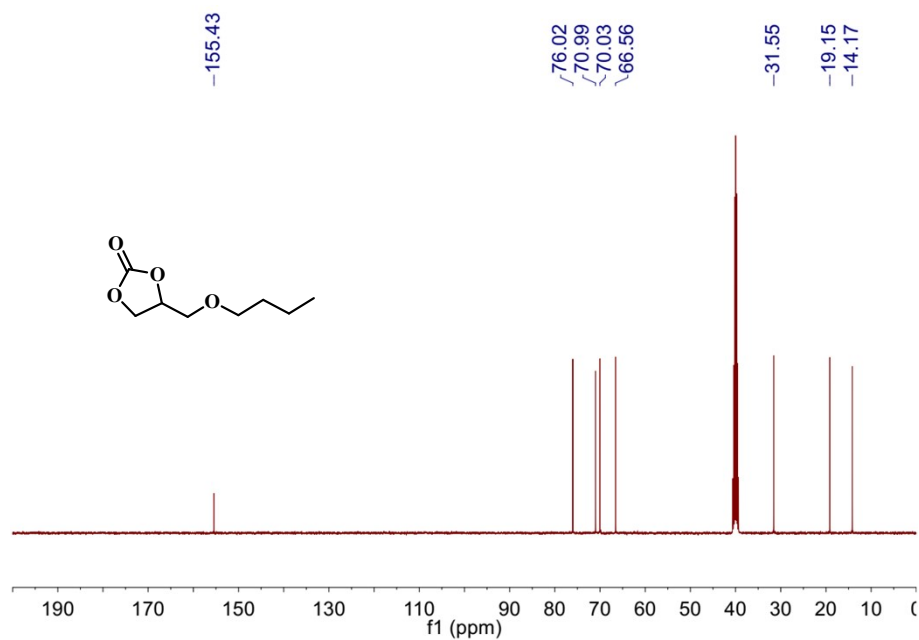
¹³C-NMR (CDCl₃)

¹³C NMR (100 MHz, CDCl₃, TMS) δ (ppm): 155.12, 133.72, 118.16, 75.13, 72.70, 68.89, 66.40.

^{1}**H-NMR** (DMSO-d$_6$)

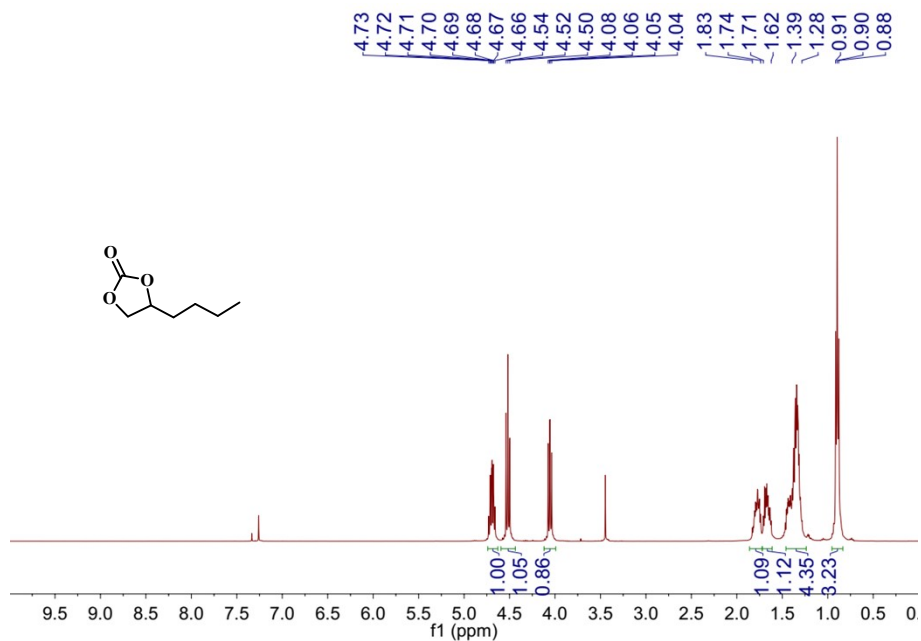^{1}H NMR (400 MHz, DMSO-d$_6$, TMS) δ (ppm): 4.91 (s, 1H), 4.51 (t, J = 8.4 Hz, 1H), 4.24 (t, J = 7.0 Hz, 1H), 3.64–3.53 (m, 2H), 3.45 (t, J = 6.4 Hz, 2H), 1.51–1.45 (m, 2H), 1.36–1.26 (m, 2H), 0.87 (t, J = 7.2 Hz, 3H).

^{13}**C-NMR** (DMSO-d$_6$)

^{13}C NMR (100 MHz, DMSO-d$_6$, TMS) δ (ppm): 155.43, 76.02, 70.99, 70.03, 66.56, 31.55, 19.15, 14.17.

¹H-NMR (CDCl₃)

¹H NMR (400 MHz, CDCl₃, TMS) δ (ppm): 4.73–4.66 (m, 1H), 4.52 (t, J = 8.2 Hz, 1H), 4.06 (dd, J = 8.4 Hz, J = 7.6 Hz, 1H), 1.83–1.74 (m, 1H), 1.71–1.62 (m, 1H), 1.39–1.28 (m, 4H), 0.90 (t, J = 7.0 Hz, 3H).

¹³C-NMR (CDCl₃)
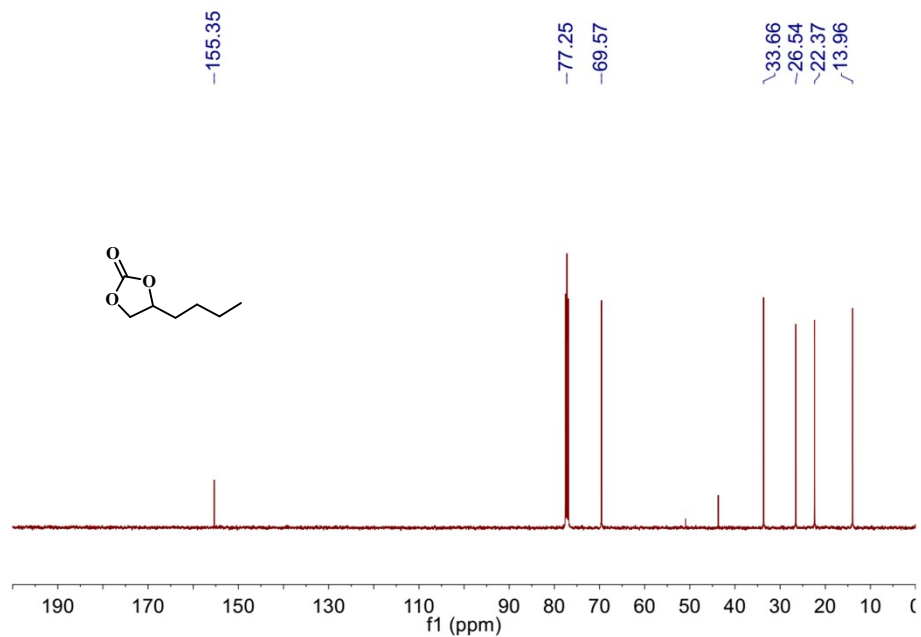
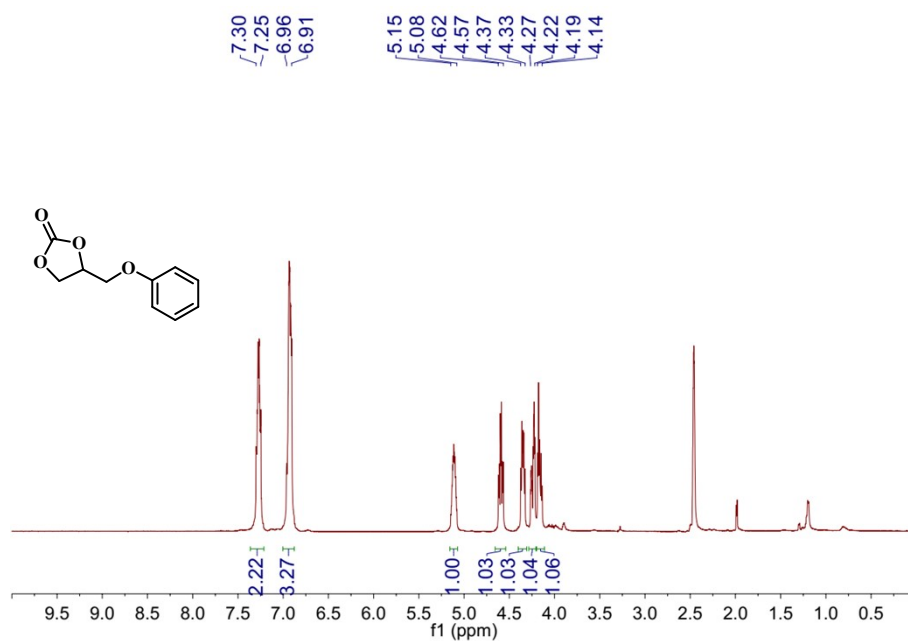¹³C NMR (100 MHz, CDCl₃, TMS) δ (ppm): 155.35, 77.25, 69.57, 33.66, 26.54, 22.37, 13.96.

¹H-NMR (DMSO-d₆)

¹H NMR (400 MHz, DMSO-d₆, TMS) δ (ppm): 7.30–7.25 (m, 2H), 6.96–6.91 (m, 3H), 5.15–5.08 (m, 1H), 4.62–4.57 (m, 1H), 4.37–4.33 (m, 1H), 4.27–4.22 (m, 1H), 4.19–4.14 (m, 1H).

¹³C-NMR (DMSO-d₆)
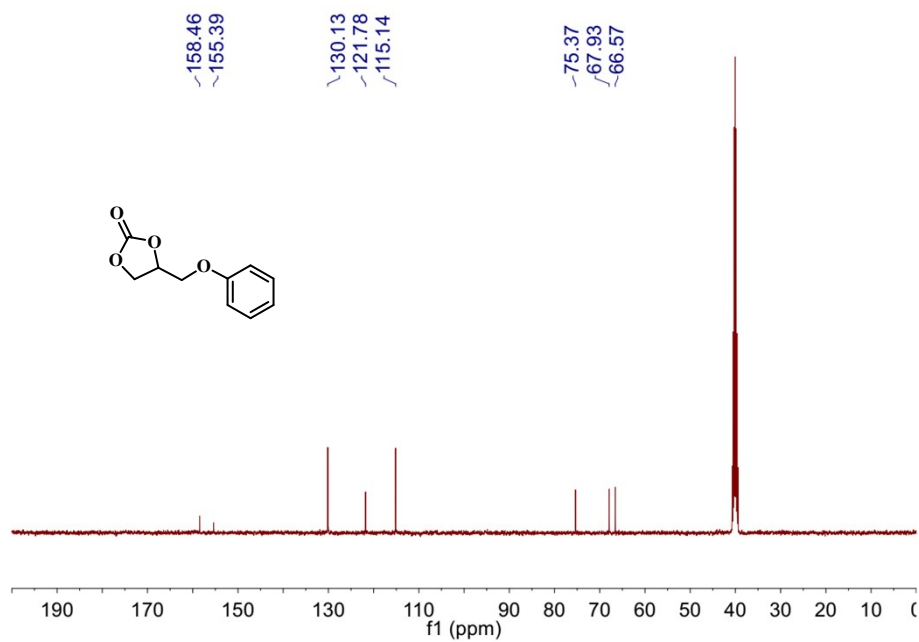
¹³C NMR (100 MHz, DMSO-d₆, TMS) δ (ppm): 158.46, 155.39, 130.13, 121.78, 115.14, 75.37, 67.93, 66.57.

9. References

1. P. D. J. Starling, P. Metilda, *J. Mol. Struct.* **2022**, *1251*, 132062.

2. V. S. Talismanov, S. V. Popkov, O. G. Karmanova, S. S. Zykova, M. V. Shustov, L. A. Zhuravleva, N. G. Tokareva, *Rasayan J. Chem.* **2021**, *14*, 1711.

3. J. Wang, W. Sng, G. Yi, Y. Zhang, *Chem. Commun.* **2015**, *51*, 12076.

4. J. Li, D. Jia, Z. Guo, Y. Liu, Y. Lyu, Y. Zhou, J. Wang, *Green Chem.* **2017**, *19*, 2675.

5. P. Puthiaraj, S. Ravi, K. Yu, W.-S. Ahn, *Appl. Catal. B Environ.* **2019**, *251*, 195.

6. J. Li, Y. Han, H. Lin, N. Wu, Q. Li, J. Jiang, J. Zhu, *ACS Appl. Mater. Interfaces* **2020**, *12*, 609.

7. Y. Sang, J. Huang, *Chem. Eng. J.* **2020**, *385*, 123973.

8. D. Jia, L. Ma, Y. Wang, W. Zhang, J. Li, Y. Zhou, J. Wang, *Chem. Eng. J.* **2020**, *390*, 124652.

9. W. Zhang, F. Ma, L. Ma, Y. Zhou, J. Wang, *ChemSusChem* **2020**, *13*, 341.

10. H. Song, Y. Wang, Y. Liu, L. Chen, B. Feng, X. Jin, Y. Zhou, T. Huang, M. Xiao, F. Huang, H. Gai, *ACS Sustainable Chem. Eng.* **2021**, *9*, 2115.

11. C. Liu, L. Shi, J. Zhang, J. Sun, *Chem. Eng. J.* **2022**, *427*, 131633.

12. J. Gu, Y. Yuan, T. Zhao, F. Liu, Y. Xu, D.-J. Tao, *Sep. Purif. Technol.* **2022**, *301*, 121971.

13. K. Cai, P. Liu, Z. Chen, P. Chen, F. Liu, T. Zhao, D.-J. Tao, *Chem. Eng. J.* **2023**, *451*, 138946.

14. H. Lyu, X. Wang, W. Sun, E. Xu, Y. She, A. Liu, D. Gao, M. Hu, J. Guo, K. Hu, J. Cheng, Z. Long, Y. Liu, P. Zhang, *Green Chem.* **2023**, *25*, 3592.

15. J. Zhang, Z.-A. Qiao, S. M. Mahurin, X. Jiang, S.-H. Chai, H. Lu, K. Nelson, S. Dai, *Angew. Chem. Int. Ed.* **2015**, *54*, 4582.

16. L. Shao, Y. Sang, N. Liu, Q. Wei, F. Wang, P. Zhan, W. Luo, J. Huang, J. Chen, *Sep. Purif. Technol.* **2021**, *262*, 118352.

17. S. Hou, J. Hu, X. Liang, D. Zhang, B. Tan, *J. Mater. Chem. A* **2022**, *10*, 15062.

18. L. Ding, N. Chanchaona, K. Konstas, M. R. Hill, X. Fan, C. D. Wood, C. H. Lau, *ChemSusChem* **2024**, e202301602.

19. C. Li, H. Cai, X. Yang, F. Liu, C. Yang, P. Chen, Z. Chen, T. Zhao, *J. CO$_2$ Util.* **2022**, *64*, 102203.

20. Y. Sang, Z. Shu, Y. Wang, L. Wang, D. Zhang, Q. Xiao, F. Zhou, J. Huang, *Appl. Surf. Sci.* **2022**, *585*, 152663.

21. D. Prasad, K. N. Patil, R. B. Dateer, H. Kim, B. M. Nagaraja, A. H. Jadhav, *Chem. Eng. J.* **2021**, *405*, 126907.

22. P. Wu, Y. Qi, Q. Li, R. Fan, S. Qin, Y. Cai, L. Yuan, W. Feng, *ACS Sustainable Chem. Eng.* **2023**, *11*, 502.

23. J. Tang, F. Wei, S. Ding, X. Wang, G. Xie, H. Fan, *Chem. Eur. J.* **2021**, *27*, 12890.

24. X.-J. Bai, X.-Y. Lu, R. Ju, H. Chen, L. Shao, X. Zhai, Y.-N. Li, F.-Q. Fan, Y. Fu, W. Qi, *Angew. Chem. Int. Ed.* **2021**, *60*, 701.

25. Z. Fang, Z. Deng, X. Wan, Z. Li, X. Ma, S. Hussain, Z. Ye, X. Peng, *Appl. Catal. B Environ.* **2021**, *296*, 120329.

26. W. Han, X. Ma, J. Wang, F. Leng, C. Xie, H.-L. Jiang, *J. Am. Chem. Soc.* **2023**, *145*, 9665.

27. J. Xu, H. Xu, A. Dong, H. Zhang, Y. Zhou, H. Dong, B. Tang, Y. Liu, L. Zhang, X. Liu, J. Luo, L. Bie, S. Dai, Y. Wang, X. Sun, Y. Li, *Adv. Mater.* **2022**, *34*, 2206991.